

# A TSUNAMI FORECAST MODEL FOR WAKE ISLAND

Diego Arcas

## Foreword

Tsunamis have been recognized as a potential hazard to United States coastal communities since the mid-twentieth century, when multiple destructive tsunamis caused damage to the states of Hawaii, Alaska, California, Oregon, and Washington. In response to these events, the United States, under the auspices of the National Oceanic and Atmospheric Administration (NOAA), established the Pacific and Alaska Tsunami Warning Centers, dedicated to protecting United States interests from the threat posed by tsunamis. NOAA also created a tsunami research program at the Pacific Marine Environmental Laboratory (PMEL) to develop improved warning products.

The scale of destruction and unprecedented loss of life following the December 2004 Sumatra tsunami served as the catalyst to refocus efforts in the United States on reducing tsunami vulnerability of coastal communities, and on 20 December 2006, the United States Congress passed the “Tsunami Warning and Education Act” under which education and warning activities were thereafter specified and mandated. A “tsunami forecasting capability based on models and measurements, including tsunami inundation models and maps.” is a central component for the protection of United States coastlines from the threat posed by tsunamis. The forecasting capability for each community described in the PMEL Tsunami Forecast Series is the result of collaboration between the National Oceanic and Atmospheric Administration office of Oceanic and Atmospheric Research, National Weather Service, National Ocean Service, National Environmental Satellite Data and Information Service, the University of Washington’s Joint Institute for the Study of the Atmosphere and Ocean, National Science Foundation, and United States Geological Survey.

## Abstract

The present study documents the development of a tsunami forecast model for Wake Island. Despite the small relevance of Wake Island as a population center, and its decreasing strategic importance in today’s political landscape, the island remains an important reference point for tsunami forecasters. Due to its geographical location, unique topography, and its large distance to any continental platform that could interfere with the tsunami signal, the tide gauge on Wake Island can provide a clean and distinct signal of the tsunami in deep water. In order to guarantee the accuracy, robustness and stability of the forecast model in an operational environment, 10 historical events have been simulated and results compared with tide gauge observations when these data were available. In addition, the robustness of the model to very large events has been tested by simulating 18 synthetic,  $M_w=9.3$  events originating at different subduction zones in the Pacific. Results from both the historical and the synthetic simulations show that Wake Island is particularly protected from tsunami impact, either by not being in the main beam of any of the events simulated or by inhibiting wave shoaling due to the absence any shallow waters in the vicinity of the island.

## 1.0 Background and Objectives

The Pacific Marine Environmental Laboratory (PMEL) of the National Oceanic and Atmospheric Administration (NOAA) Center for Tsunami Research (NCTR) has developed a tsunami forecasting capability for operational use by NOAA's two Tsunami Warning Centers located in Hawaii and Alaska (Titov et al. 2005). The system is designed to efficiently provide basin-wide warning of approaching tsunami waves. The system termed Short-term Inundation Forecast of Tsunamis (SIFT) combines real-time tsunami event data with numerical models to produce estimates of tsunami wave arrival times and amplitudes at a coastal community of interest. The SIFT system integrates several key components: deep-ocean, real-time observations of tsunamis, a basin-wide pre-computed propagation database of water level and flow velocities based on potential seismic unit sources, an inversion algorithm to refine the tsunami source based on deep-ocean observations during an event, and optimized tsunami forecast models.

Wake Island is an unincorporated territory of the United States located approximately 3,700 km (2,300 mi) west of the Hawaiian Islands. Its use is restricted to military operations and there are no indigenous or permanent residents on the island.

"The United States annexed Wake Island in 1899 for the site of a cable station. An air and naval base was constructed from 1940-41, and in December of 1941, the island was captured by the Japanese and held until the end of World War II. In the following years, the U.S. military developed Wake Island as a refueling and emergency landing site for military and commercial aircraft transiting the Pacific. In August 2006, the approach of category 5 typhoon Ioke called for an evacuation of personnel, and the major damage caused by its sustained winds of 250 kph and 6 m storm surge halted subsequent operations. A small military contingent along with 75 contractor personnel has since returned to the island to conduct clean up and restoration". (source: Central Intelligence Agency World Fact Book).

Wake Island was one of the locations selected for the development of a tsunami warning model because despite the limited human presence on the island, its low-lying topography makes it nearly impossible for the island residents to find shelter from large tsunami waves. A tsunami forecast model for the island would provide residents with timely and vital information to determine the best course of action in the event of a tsunami.

It can also be argued that the location of Wake Island, with its unique and deep bathymetric surroundings, provides an ideal opportunity for Tsunami Warning Centers to gauge propagating tsunami waves in deep water. In this regard, the absence of a continental shelf or any other surrounding islands will minimize the interaction of the tsunami wave with the local bathymetry, allowing the island's tide gauge to perform almost as an additional Deep-water Assessment and Reporting of Tsunamis (DART) system.

The existence of an NOS tide gauge on the island, established on May 29, 1950 and operated by a National Weather Service office located at the U.S. Army Base is crucial for the development of a tsunami forecast model, since it provides historical data for model validation and the possibility of quantitative assessment of model accuracy and performance in future events.

This report details the development of a high-resolution tsunami forecast model for Wake Island, including development of the bathymetric grids, model validation with historic events, and stability testing with a set of synthetic mega-tsunami events (Mw 9.3). Inundation results from such artificial events are also presented in later sections.

## 2.0 Forecast Methodology

A high-resolution inundation model was used as the basis for the operational forecast model to provide

an estimate of wave arrival time, height, and inundation immediately following tsunami generation. Tsunami forecast models are run in real time while the tsunami in question is propagating across the open ocean. These models are designed and tested to perform under very stringent time constraints given that time is generally the single limiting factor in saving lives and property. The goal is to maximize the amount of time that an at-risk community has to respond to the tsunami threat by providing timely and accurate information.

The tsunami forecast model, based on the Method of Splitting Tsunami (MOST), emerges as the solution in the SIFT system by modeling real-time tsunamis in minutes while employing high-resolution grids constructed by the National Geophysical Data Center or, in limited instances, internally. Each forecast model consists of three telescoped grids with increasing spatial and temporal resolution for simulation of wave inundation onto dry land. The forecast model utilizes the most recent bathymetry and topography available to reproduce the correct wave dynamics during the inundation computation. Forecast models are constructed for at-risk populous coastal communities in the Pacific and Atlantic Oceans. Previous and present development of forecast models in the Pacific (Titov *et al.*, 2005; Titov, 2009; Tang *et al.*, 2009; Wei *et al.*, 2008) have validated the accuracy and efficiency of the forecast models currently implemented in the SIFT system for real-time tsunami forecast. The model system is also a valuable tool in hind-cast research. Tang *et al.* (2009) provides forecast methodology details.

### **3.0 Model Development**

Modeling of coastal communities is accomplished by development of a set of three nested grids that telescope down from a large spatial extent to a grid that finely defines the localized community. The basis for these grids is a high-resolution digital elevation model constructed by either NCTR or, more commonly, by the National Geophysical Data Center (NGDC) using best available bathymetric, topographic, and coastal shoreline data for an at-risk community. For each community, data are compiled from a variety of sources to produce a digital elevation model referenced to Mean High Water in the vertical and to the World Geodetic System 1984 in the horizontal (<http://ngdc.noaa.gov/mgg/inundation/tsunami/inundation.html>). From these digital elevation models, a set of three high-resolution reference models are constructed and then “optimized” to run in an operationally specified period of time.

### 3.1 Forecast Area

“Wake Island is an atoll comprised of three islets in the central Pacific Ocean. The three islets Wilkes, Peale, and Wake are connected by causeways and sit on a 7.2 km (4.5 mile) long, 3.2 km (2 mile) wide reef enclosing a lagoon that is also the crater of an underwater volcano. Their total land area is 6.5 square km (2.5 square miles) and the maximum elevation is 6 meters (21 feet) above sea level. **Figure 1** is a map of Wake Island, showing the relative position of the three islets and the location of the island’s tide gauge between Wilkes and Wake Island”. (source: Encyclopedia Britannica)

### 3.2 Historical Events and Data

The tide gauge on Wake Island was installed on May 29, 1950 and re-deployed at its current location ( $166.6177^{\circ}$  E,  $19.2906^{\circ}$  N) along the small boat channel on the southern coast of the island on January 20, 1989. Acceptable quality tide gauge from the Wake Island tide gauge was found for 4 of the 10 historic events (see **Table 1**) used in the validation of the tsunami model for the island. The tsunami events for which model results are compared with tide gauge data in this report are: Kuril 1994, Andreanof 1996, Kuril 2006 and Kuril 2007. For the other listed events, the data were either not available or the signal to noise ratio of the time series was too low to accurately identify the tsunami.

The results of modeling a large number of events in Wake Island suggest that the island is relatively well protected from tsunami inundation, either due to its small size and deep bathymetric surroundings or to the presence of a coral reef that almost completely encloses the island, but most likely to both of these. Few of the tested events and none of the historical ones have caused significant inundation on the island. Moreover, neither of the two largest historical events in the Pacific Ocean since the inception of tide gauge operations at Wake Island, the 1960 Chile and 1964 Gulf of Alaska events, showed large tsunami waves at the gauge. Waves from the 1964 event were in the order of 20-30 cm (peak-to-trough) whereas those for the 1960 event show maximum wave heights of approximately 80 cm. These two events have not been included in the list of simulated historical tsunamis due to the lack of reliable tsunami sources for them; however, their recorded tide gauge data is presented in **Figures C.1 and C.2** (Appendix C) for reference.

### 3.3 Model Setup

Setup of the computational grids for the Method of Splitting Tsunami code (Titov, 1998) requires a total of 3 nested grids for which the outer grid A has the lowest spatial resolution, but covers the largest area, and the inner grid C has the highest spatial resolution, but covers a reduced geographical area. The code makes use of an additional intermediate grid B with medium resolution and spatial coverage. Each interior grid is fully enclosed in the area covered by its immediate exterior grid, and inundation is computed only in the most interior grid (Grid C). The purpose of the set of three nested grids is to ensure that as the tsunami wavelength shrinks when it travels from deep to shallow waters, the model maintains an approximately constant number of grid nodes per wavelength.

During the development of an operational forecast model, a higher resolution set of grids referred to as the reference model is generated first. The purpose of the reference model is to evaluate grid convergence between a high resolution model and the forecast model, ensuring that the solution obtained with the lower resolution forecast model is consistent with that computed with the high

resolution reference model.

In the case of Wake Island, due to the absence of a continental shelf, the tsunami will most likely not shorten its wavelength significantly until it reaches the immediate vicinity of the island. Because there are no neighboring coastlines for the tsunami to interact with, there is, therefore, no need for extensive area coverage with A or B grids. However, due to the presence of a shallow coral reef responsible for the generation of high frequency waves surrounding the island, the resolution of grid B was kept relatively high, 3 arc seconds, even in the forecast model. An effort was made to include almost the entire island within the C grid of the forecast model; however, due to the large area covered by the island and its surrounding reef, the need to maintain a relatively high grid resolution, and the limited amount of processing time to execute an operational forecast model, a decision was made to center the forecast grid C around the tide gauge location, resulting in the exclusion of part of the coral reef on the western side of the island.

Because reference grid A was designed with smaller coverage than normal due to the absence of a continental shelf, the same grid A was used for both the reference and the forecast model without any modification.

**Figure 2** shows an aerial view of Wake Island and **Figures 3 and 4** show grid areas and relative position with respect to the island for the reference and forecast models. **Table 2** summarizes the parameters and model set up for each set of grids.

The original bathymetric and topographic grid data used in the development of the Wake Island model were provided by the National Geophysical Data Center (NGDC) under PMEL contract. Details of data gathering and grid construction techniques used by NGDC in the generation of the original grid are provided by Medley *et al*, (Medley, 2009).

## 4.0 Results and Discussion

Three types of tests were performed to assess the forecast model convergence, accuracy and robustness characteristics. For convergence, results obtained with the reference model were compared with those obtained with the forecast model to confirm consistency of results at least for the leading tsunami waves. This type of test is not, strictly speaking, a grid convergence test in the sense used in computational science, since the solution is compared on grids with varying resolution, coverage and bathymetric information; however, it provides a good estimate of the similarities and discrepancies between the solutions of a more accurate, high resolution model of the area and that of a run-time optimized forecast model.

The accuracy of both the reference and the forecast models is evaluated by comparing modeled and recorded data for a set of historical events.

Robustness tests include the simulation of 18 tsunamis from Mw 9.3 earthquakes around the Pacific basin. **Figures 5 and 6** show the epicenter of the historical events and center of the rupture segment for each of these artificial events, respectively. The forecast model was required to run smoothly without instabilities during 24 hours of simulation for each of these synthetic mega events.

### 4.1 Model Validation

Model validation using historical events is typically done by comparing the modeled signal with the

signal recorded by the tide gauge. In the case of Wake Island, the tide gauge is located in a small boat harbor on the south side of the island. The harbor is connected to the open ocean by an approximately 30 m wide, 450 m long channel. Tsunami wave dynamics were hard to capture inside the small boat harbor even at 1/3 arc sec ( $\sim 10$  m) reference grid resolution, most likely due to the difficulty in representing the narrow channel. At forecast model resolution 1 arc second ( $\sim 30$  m), no more than 1 grid node is available to capture the width of the channel. Consequently, an additional time series located outside the small boat harbor at the entrance of the channel (166.6140 E 19.2895 N), and referred to henceforth as sample point 2, was selected for comparison.

Comparison results at the tide station for the reference and forecast models are presented in **Figures 7 through 16** with Figures 8, 9, 12 and 13 also displaying tide gauge data for those events. Plots of the comparison at sample point 2 are shown in **Figures D.1 through D.10**. The results reflect an almost peak-to-peak agreement between the forecast and reference models in most cases. This comparison is particularly good in water level signals taken at sample point 2. The events that resulted in the largest discrepancies between the reference and forecast models were the 1946 Unimak, showing approximately 20% discrepancy in the maximum amplitude of the signal, but almost peak-to-peak correlation even in later waves, and the 2007 Kuril, 2003 Rat Island, and 2006 Tonga with good max amplitude correlation, but some discrepancies in the simulation of later waves.

Assessment of the accuracy of both the forecast and reference model was examined for the 1994 Kuril, 1996 Andreanof, 2006 Kuril, and 2007 Kuril in Figures 8, 9, 12 and 13. For all these cases except 2006 Kuril, both the reference and model series were able to capture the arrival time, wave period and overall magnitude of the event. Results for the 2006 Kuril Is. event showed wave amplitudes approximately half the size of those recorded at the tide gauge. Despite the need for higher resolution grids to accurately resolve wave dynamics inside the harbor, tide gauge comparisons with modeled data turned out to be in better agreement inside the harbor than at sample point 2 at the entrance of the channel. This is probably due to the proximity of the sample point to the tide gauge sensor, overriding the lack of resolution in wave dynamics inside the harbor.

In addition to tide gauge comparisons, maximum sea level elevation at each point on the grid for every event simulated were computed and compared between the reference and forecast models. **Figures 17 through 26** show similarities and discrepancies between models for each historical scenario. Agreement on the southern section of the island was in general very good. However, the area surrounding the entrance channel to the internal lagoon and separating Peale from Wake Island seems to display consistently low values in the forecast runs when compared with the reference runs. A possible solution to this effect could be the extension of the intermediate grid B further North, but this possibility has not been investigated.

## 4.2 Model Stability Testing using Synthetic Scenarios

During model stability testing, 18 mega tsunamis (earthquake Mw 9.3) were simulated using the forecast model. Details of the 18 synthetic events tested can be found in **Table 3**. Each of these extreme synthetic events is constructed along a 1000 km long and 100 km wide fault plane with uniform slip amount of 29 m along the fault. The output from the code at every time step was visualized and inspected for instabilities. The cause of any instability was corrected and a final set of forecast grids emerged from the process. As in the case of historical events, the maximum water elevation at every point in the computational grid was recorded for each scenario. Although the original purpose of the stability tests is not to provide hazard assessment for the island, it is important

to notice that the maximum wave height tends to occur inside the small boat harbor. The highest sea level elevation recorded at this point was 1.4 m (wave amplitude) and occurred for synthetic scenario 1, originating in the Kuril Islands. None of the mega events tested on the grids generated substantial flooding on the island. Results are presented in **Figures 27 to 44**. Time series of the tsunami signal at the Wake Island's tide gauge for the 18 synthetic Mw=9.3 events can be found in **Figures E1 through E3** in Appendix E.

In addition to the eighteen Mw=9.3 events, the stability of the model to very small events is also tested by making sure that no spurious oscillations develop during the simulation of small Mw=7.3 event. For this particular study the small event was selected off the coast of Chile and was generated by rupture of a single unit source with a slip amount of 0.5 meters. This source appears listed in **Table 3** as synthetic case 0. During the simulation of this event, no unphysical oscillations were observed. Results showing the maximum water elevation at every point for this event are reflected in **Figure 45**.

## 5.0 Summary and Conclusion

A set of tsunami forecast grids have been developed for operational use by the Tsunami Warning Centers in conjunction with the Method of Splitting Tsunami code. Two sets of grids were developed: a high resolution set intended to provide reference values, and a forecast set designed to minimize processor run time and to provide real time tsunami estimates on Wake Island.

During model development, some geographical characteristics unique to Wake Island, such as the presence of a coral reef and the absence of shallow areas near the island were factored into the grid design. After simulation of 10 historical events and 18 synthetic events, it becomes evident that these unique geographical features may be attenuating the impact of a tsunami on the island. The absence of shallow areas in the neighborhood of the island probably prevents the wave from shoaling and gaining elevation as it approaches the coastline, and the presence of a coral reef surrounding the island serves as a natural break-water, reflecting part of the tsunami energy away from the island. Minimum inundation was observed on the island, most of it located in the narrow channels separating Peale from Wake and Wilkes islands.

The presence of the shallow coral reef, however, makes it impossible to sub-sample the grid significantly while still resolving high frequency waves generated by the reef. This resulted in Wake Island being one of the highest resolution forecast models developed, translating into longer execution time, resulting in 4 hours of simulation time performed in just over 15 minutes on an Intel Xeon 3.6 GHz processor.

## 6.0 Acknowledgments

This research is funded by the NOAA Center for Tsunami Research (NCTR). The authors would like to thank the modeling group of NCTR for their helpful suggestions and discussions. This publication is partially funded by the Joint Institute for the Study of the Atmosphere and Ocean (JISAO) under NOAA cooperative agreement No. NA17RJ1232, JISAO Contribution No. This is PMEL contribution No.

## 7.0 References

Medley, P.R., L.A. Taylor, B.W. Eakins, K.S. Carignan, R.R. Warnken, and E. Lim (2009): Digital Elevation Models of Wake Island: Procedures, Data Sources and Analysis. NGDC Technical Memo.

Titov, V.V., and C.E. Synolakis (1998): Numerical modeling of tidal wave runup. *J. Waterw. Port Coast. Ocean Eng.*, 124(4), 157–171.

Titov, V.V., F.I. González, E.N. Bernard, M.C. Eble, H.O. Mofjeld, J.C. Newman, and A.J. Venturato (2005): Real-time tsunami forecasting: Challenges and solutions. *Nat. Hazards*, 35(1), Special Issue, U.S. National Tsunami Hazard Mitigation Program, 41-58.

Titov, V.V. (2009): Tsunami forecasting. In *The Sea*, Vol. 15, Chapter 12, Harvard University Press, Cambridge, MA, and London, England, 371–400.

Tang, L., V.V. Titov, and C.D. Chamberlin (2009): Development, testing, and applications of site-specific tsunami inundation models for real-time forecasting. *J. Geophys. Res.*, 6, doi: 10.1029/2009JC005476, in press.

Wei, Y., E. Bernard, L. Tang, R. Weiss, V. Titov, C. Moore, M. Spillane, M. Hopkins, and U. Kânoglu (2008): Real-time experimental forecast of the Peruvian tsunami of August 2007 for U.S. coastlines. *Geophys. Res. Lett.*, 35, L04609, doi: 10.1029/2007GL032250.

*Encyclopædia Britannica. Encyclopædia Britannica Online.* Encyclopædia Britannica, 2010. Web. 2 2010 <<http://search.eb.com/eb/article-9075898>>.

Central Intelligence Agency. The World Fact Book. <https://www.cia.gov/library/publications/the-world-factbook/geos/wq.html>



## List of Tables

**Table 1:** Historical tsunami events in the Pacific Ocean considered in this report.

**Table 2.** MOST setup parameters for reference and forecast models.

**Table 3.** Description of the synthetic tsunami scenarios.

## List of Figures

**Figure 1:** Geographic map of the Wake Island area showing the relative position of the three islands in the atoll (contour lines every 100 m.).

**Figure 2:** Aerial view of Wake Island taken from the Northwest with the causeway between Peale and Wake Islets to the right of the image.

**Figure 3:** Map of the Wake Island atoll showing the relative position of the reference model grids.

**Figure 4:** Map of the Wake Island atoll showing the relative position of the forecast model grids.

**Figure 5:** Location of the 10 historical events used in the model validation tests, showing the relative position of Wake Island to the epicenter locations.

**Figure 6:** Location of the mid-rupture point of the 18 synthetic ( $M_w=9.3$ ) events used in the model robustness tests, showing the relative position of Wake Island to the epicenter locations.

**Figure 7:** Comparison at the Wake Island tide gauge of the forecast and reference models for the 1946 Unimak Is. tsunami.

**Figure 8:** Comparison at the Wake Island tide gauge of the forecast and reference models for the 1994 Kuril Is. tsunami with observed data.

**Figure 9:** Comparison at the Wake Island tide gauge of the forecast and reference models for the 1996 Andreanof Is. tsunami with observed data.

**Figure 10:** Comparison at the Wake Island tide gauge of the forecast and reference models for the 2003 Rat Is. tsunami.

**Figure 11:** Comparison at the Wake Island tide gauge of the forecast and reference models for the 2006 Tonga tsunami.

**Figure 12:** Comparison at the Wake Island tide gauge of the forecast and reference models for the 2006 Kuril Is. tsunami with observed data.

**Figure 13:** Comparison at the Wake Island tide gauge of the forecast and reference models for the 2007 Kuril Is. tsunami with observed data.

**Figure 14:** Comparison at the Wake Island tide gauge of the forecast and reference models for the 2007 Solomon Is. tsunami.

**Figure 15:** Comparison at the Wake Island tide gauge of the forecast and reference models for the 2007 Peru tsunami.

**Figure 16:** Comparison at the Wake Island tide gauge of the forecast and reference models for the 2007 Chile tsunami.

**Figure 17:** Maximum sea surface elevation computed with the reference (left) and forecast (right) models for the 1946 Unimak Is. tsunami.

**Figure 18:** Maximum sea surface elevation computed with the reference (left) and forecast (right) models for the 1994 Kuril Is. tsunami.

**Figure 19:** Maximum sea surface elevation computed with the reference (left) and forecast (right) models for the 1996 Andreanof Is. tsunami.

**Figure 20:** Maximum sea surface elevation computed with the reference (left) and forecast (right) models for the 2003 Rat Is. tsunami.

**Figure 21:** Maximum sea surface elevation computed with the reference (left) and forecast (right) models for the 2006 Tonga Is. tsunami.

**Figure 22:** Maximum sea surface elevation computed with the reference (left) and forecast (right) models for the 2006 Kuril Is. tsunami.

**Figure 23:** Maximum sea surface elevation computed with the reference (left) and forecast (right) models for the 2007 Kuril Is. tsunami.

**Figure 24:** Maximum sea surface elevation computed with the reference (left) and forecast (right) models for the 2007 Solomon Is. tsunami.

**Figure 25:** Maximum sea surface elevation computed with the reference (left) and forecast (right) models for the 2007 Peru tsunami.

**Figure 26:** Maximum sea surface elevation computed with the reference (left) and forecast (right) models for the 2007 Chile tsunami.

**Figure 27:** Maximum sea surface elevation computed with the forecast models for synthetic scenario 1 ( $M_w=9.3$ ).

**Figure 28:** Maximum sea surface elevation computed with the forecast models for synthetic scenario 2 ( $M_w=9.3$ ).

**Figure 29:** Maximum sea surface elevation computed with the forecast models for synthetic scenario 3 ( $M_w=9.3$ ).

**Figure 30:** Maximum sea surface elevation computed with the forecast models for synthetic scenario 4 ( $M_w=9.3$ ).

**Figure 31:** Maximum sea surface elevation computed with the forecast models for synthetic scenario 5 ( $M_w=9.3$ ).

**Figure 32:** Maximum sea surface elevation computed with the forecast models for synthetic scenario 6 ( $M_w=9.3$ ).

**Figure 33:** Maximum sea surface elevation computed with the forecast models for synthetic scenario 7 ( $M_w=9.3$ ).

**Figure 34:** Maximum sea surface elevation computed with the forecast models for synthetic scenario 8 ( $M_w=9.3$ ).

**Figure 35:** Maximum sea surface elevation computed with the forecast models for synthetic scenario 9 ( $M_w=9.3$ ).

**Figure 36:** Maximum sea surface elevation computed with the forecast models for synthetic scenario 10 ( $M_w=9.3$ ).

**Figure 37:** Maximum sea surface elevation computed with the forecast models for synthetic scenario 11 ( $M_w=9.3$ ).

**Figure 38:** Maximum sea surface elevation computed with the forecast models for synthetic scenario 12 ( $M_w=9.3$ ).

**Figure 39:** Maximum sea surface elevation computed with the forecast models for synthetic scenario 13 ( $M_w=9.3$ ).

**Figure 40:** Maximum sea surface elevation computed with the forecast models for synthetic scenario 14 ( $M_w=9.3$ ).

**Figure 41:** Maximum sea surface elevation computed with the forecast models for synthetic scenario 15 ( $M_w=9.3$ ).

**Figure 42:** Maximum sea surface elevation computed with the forecast models for synthetic scenario 16 ( $M_w=9.3$ ).

**Figure 43:** Maximum sea surface elevation computed with the forecast models for synthetic scenario 17 ( $M_w=9.3$ ).

**Figure 44:** Maximum sea surface elevation computed with the forecast models for synthetic scenario 18 ( $M_w=9.3$ ).

**Figure 45:** Maximum sea surface elevation computed with the forecast models for the small synthetic micro scenario 18 ( $M_w=6.8$ ).

**Figure C.1:** Recorded tide gauge record at Wake Island during the 1960 Chile tsunami.

**Figure C.2:** Recorded tide gauge record at Wake Island during the 1964 Prince William Sound tsunami.

**Figure D.1:** Comparison at the Wake Island sample point 2 of the forecast and reference models for the 1946 Unimak Is. tsunami.

**Figure D.2:** Comparison at the Wake Island sample point 2 of the forecast and reference models for the 1994 Kuril Is. tsunami.

**Figure D.3:** Comparison at the Wake Island sample point 2 of the forecast and reference models for the 1996 Andreanof Is. tsunami.

**Figure D.4:** Comparison at the Wake Island sample point 2 of the forecast and reference models for the 2003 Rat Is. tsunami.

**Figure D.5:** Comparison at the Wake Island sample point 2 of the forecast and reference models for the 2006 Tonga Is. tsunami.

**Figure D.6:** Comparison at the Wake Island sample point 2 the forecast and reference models for the 2006 Kuril Is. tsunami.

**Figure D.7:** Comparison at the Wake Island sample point 2 the forecast and reference models for the 2007 Kuril Is. tsunami.

**Figure D.8:** Comparison at the Wake Island sample point 2 the forecast and reference models for the 2007 Solomon Is. tsunami.

**Figure D.9:** Comparison at the Wake Island sample point 2 the forecast and reference models for the 2007 Peru Is. tsunami.

**Figure D.10:** Comparison at the Wake Island sample point 2 the forecast and reference models for the 2007 Chile Is. tsunami.

**Figure E.1:** Recorded tide gauge record at Wake Island for synthetic scenarios 1 through 6.

**Figure E.2:** Recorded tide gauge record at Wake Island for synthetic scenarios 7 through 12.

**Figure E.2:** Recorded tide gauge record at Wake Island for synthetic scenarios 13 through 18.

#### List of Tables

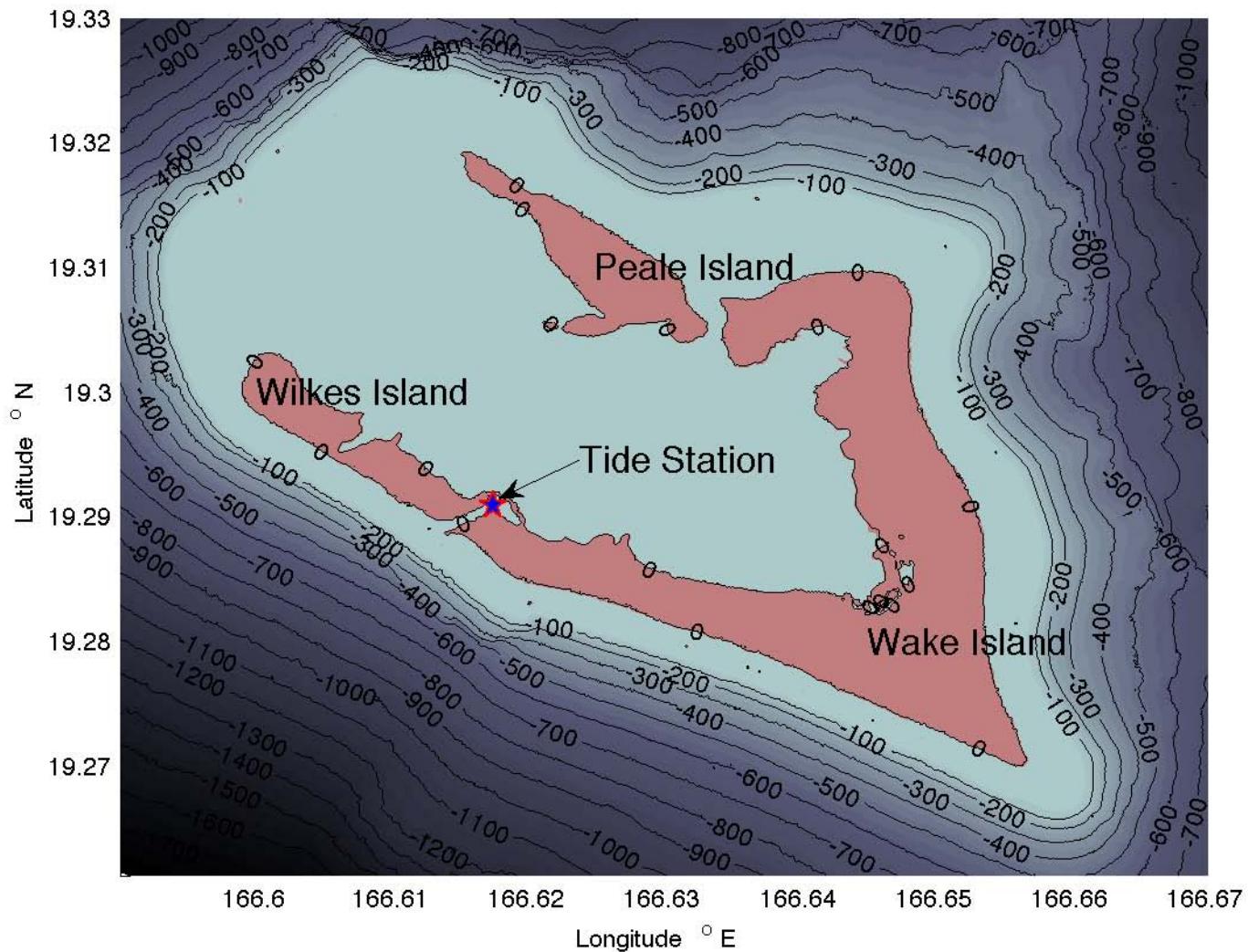
- 1 Historical events used for model validation for Wake Island
- 2 MOST setup parameters for reference and forecast models for Wake Island
- 3 Synthetic tsunami sources used in the forecast model robustness test for Wake Island

Event	Date	Zone	M <sub>w</sub>	Lon(°)	Lat(°)	Source
1946 Unimak	1946.04.01	ACSZ	8.1	163.19W	53.32N	1.6×b22+8.4×b23+17.8×b24
1994 Kuril	1994.10.04	KISZ	8.1	147.32E	43.70N	9.0×a20
1996 Andreanof	1996.06.10	ACSZ	7.9	177.63W	51.56N	2.4×a15+0.8×b16
2003 Rat Island	2003.11.17	ACSZ	7.8	178.74E	51.13N	2.81×b11
2006 Tonga	2006.05.03	NZKT	8.1	174.16W	20.13N	8.44×b29
2006 Kuril	2006.11.15	KISZ	8.1	154.32E	46.75N	4.0×a12+0.5×b12 +2.0×a13+1.5×b13
2007 Kuril	2007.01.13	KISZ	7.9	154.80E	46.18N	-3.82×b13
2007 Solomon	2007.04.01	NTSZ	8.2	156.4E	7.96S	12.0×b10
2007 Peru	2001.06.23	CSSZ	8.0	73.31W	16.14S	0.9×a61+1.25×b61 +5.6×a62+6.97×b62+3.5×z62
2007 Chile	2007.11.14	CSSZ	7.7	69.9W	22.2S	1.65×z73

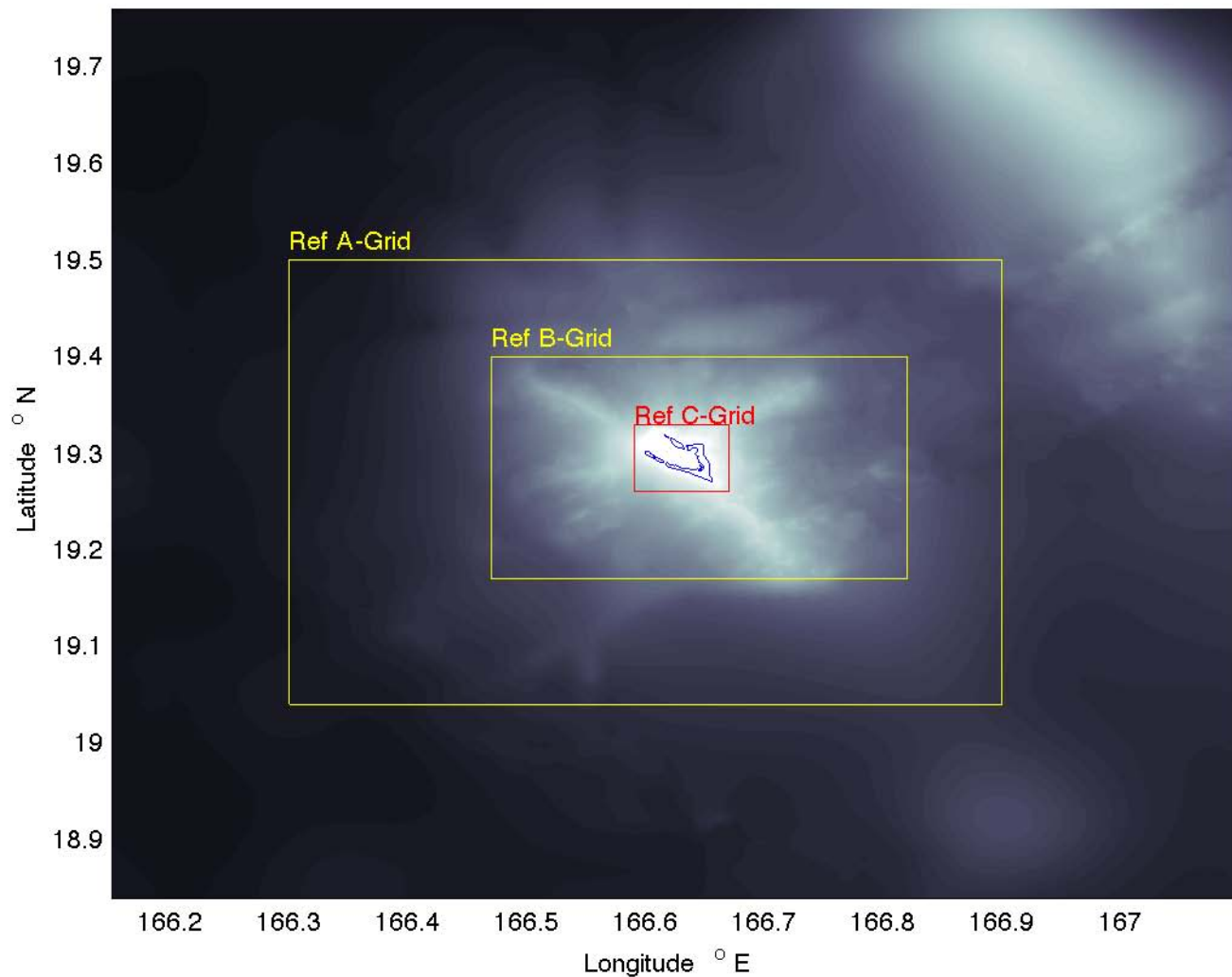
Model Setup	Reference Model			Forecast Model		
	Grid A	Grid B	Grid C	Grid A	Grid B	Grid C
W	E166.30	E166.470	E166.5901	E166.30	E166.5525	E166.6069
E	E166.90	E166.820	E166.6701	E166.90	E166.7192	E166.6546
S	N19.50	N19.40	N19.33	N19.50	N19.3358	E19.3109
N	N19.05	N19.17	N19.2613	N19.05	N19.2433	E19.2731
$dx$	30"	3"	1/3"	30"	3"	1"
$dy$	30"	3"	1/3"	30"	3"	1"
$nx \times ny$	73x55	421x277	865x743	73x55	201x112	173x137
$dt$ (sec)	3.5	0.3	0.07	3.24	0.54	0.27
$D_{min}$	5 m			1 m		
Fric. ( $n^2$ )	0.00125			0.00125		
CPU Time	~ 7 min for 4-hour simulation			~ 16 min for 4-hour simulation		
Warning Pt.	E166.6175, N19.2910					

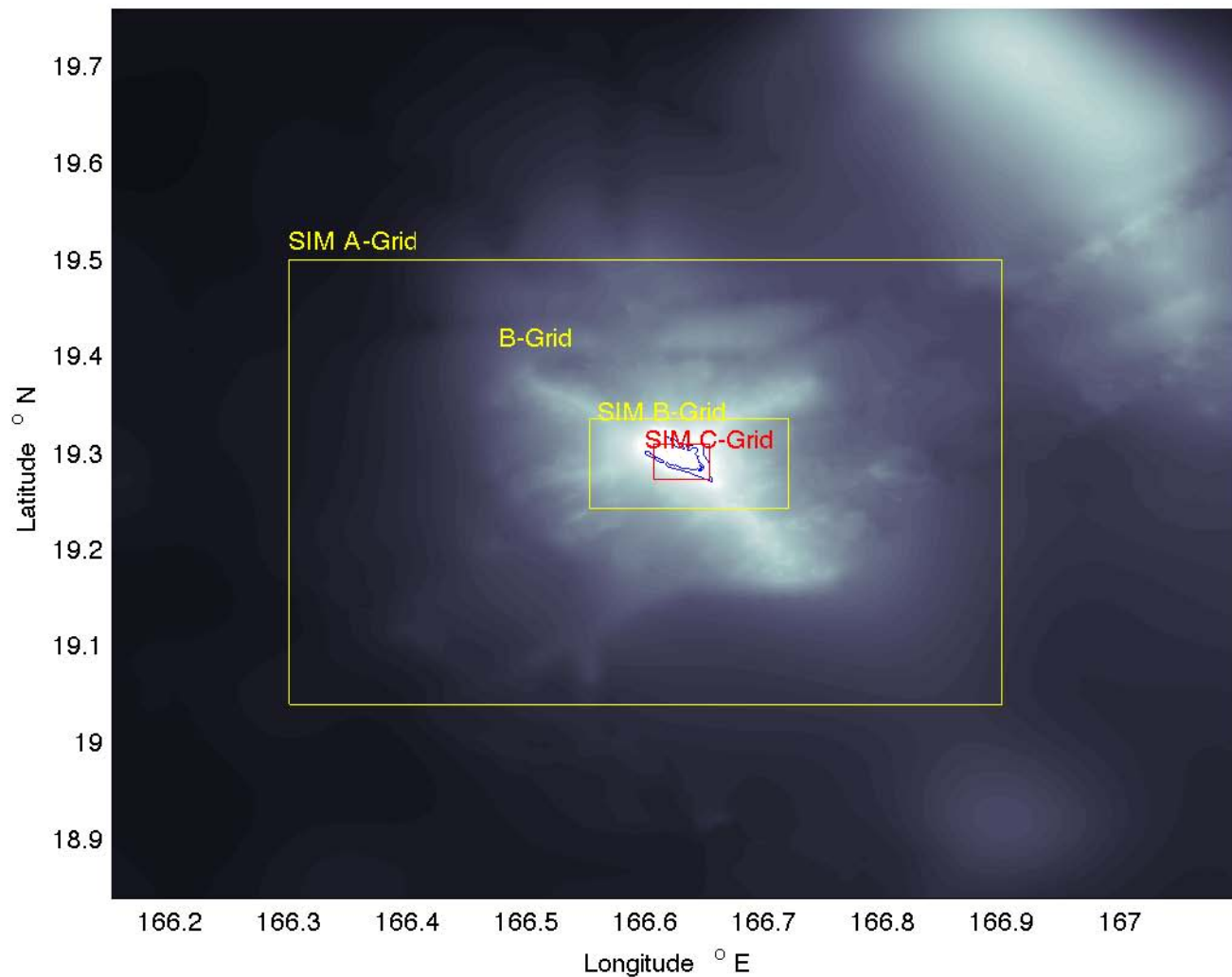
Scenario Name	Source Zone	Tsunami Source	$\alpha$ [m]
<b>Mega-tsunami Scenario</b>			
KISZ 22-31	Kamchatka-Yap-Mariana-Izu-Bonin	A22-A31, B22-B31	29
KISZ 1-10	Kamchatka-Yap-Mariana-Izu-Bonin	A1-A10, B1-B10	29
ACSZ 12-21	Aleutian-Alaska-Cascadia	A12-A21, B12-B21	29
ACSZ 22-31	Aleutian-Alaska-Cascadia	A22-A31, B22-B31	29
ACSZ 38-47	Aleutian-Alaska-Cascadia	A38-A47, B38-B47	29
ACSZ 56-65	Aleutian-Alaska-Cascadia	A56-A65, B56-B65	29
CSSZ 1-10	Central and South America	A1-A10, B1-B10	29
CSSZ 37-46	Central and South America	A37-A46, B37-B46	29
CSSZ 92-101	Central and South America	A92-A101, B92-B101	29
CSSZ 64-73	Central and South America	A64-A73, B64-B73	29
NTSZ 20-29	New Zealand-Kermadec-Tonga	A20-A29, B20-B29	29
NTSZ 30-39	New Zealand-Kermadec-Tonga	A30-A39, B30-B39	29
NVSZ 28-37	New Britain-Solomons-Vanuatu	A28-A37, B28-B37	29
MOSZ 1-10	ManusOCB	A1-A10, B1-B10	29
NGSZ 3-12	North New Guinea	A3-A12, B3-B12	29
EPSZ 6-15	East Philippines	A6-A15, B6-B15	29
RNSZ 12-21	Ryukus-Kyushu-Nankai	A12-A21, B12-B21	29
KISZ 32-41	Kamchatka-Yap-Mariana-Izu-Bonin	A32-A41, B32-B41	29
<b>Micro-tsunami Scenario</b>			
CSSZ B88	Central and South America	B88	0.1

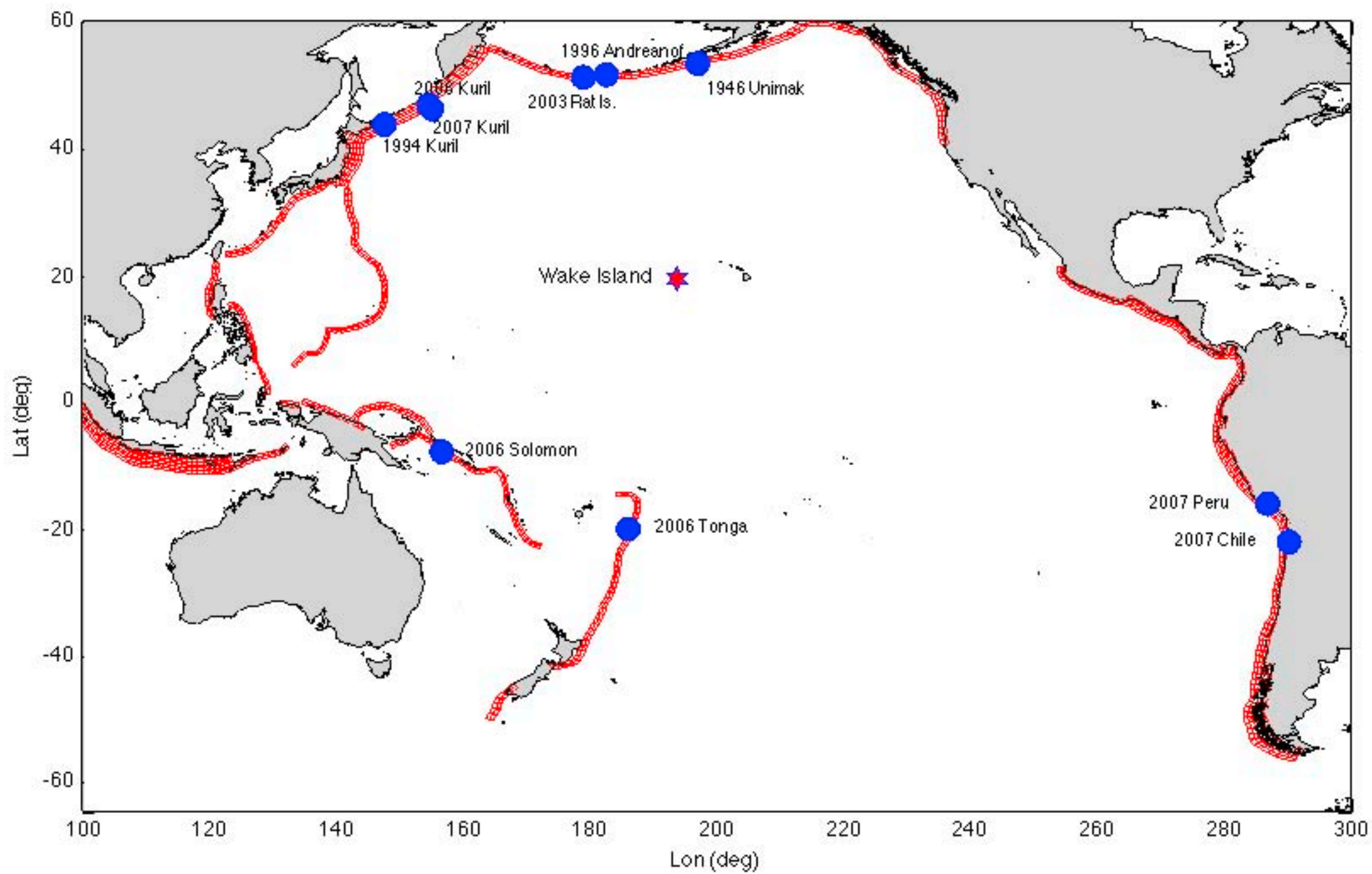




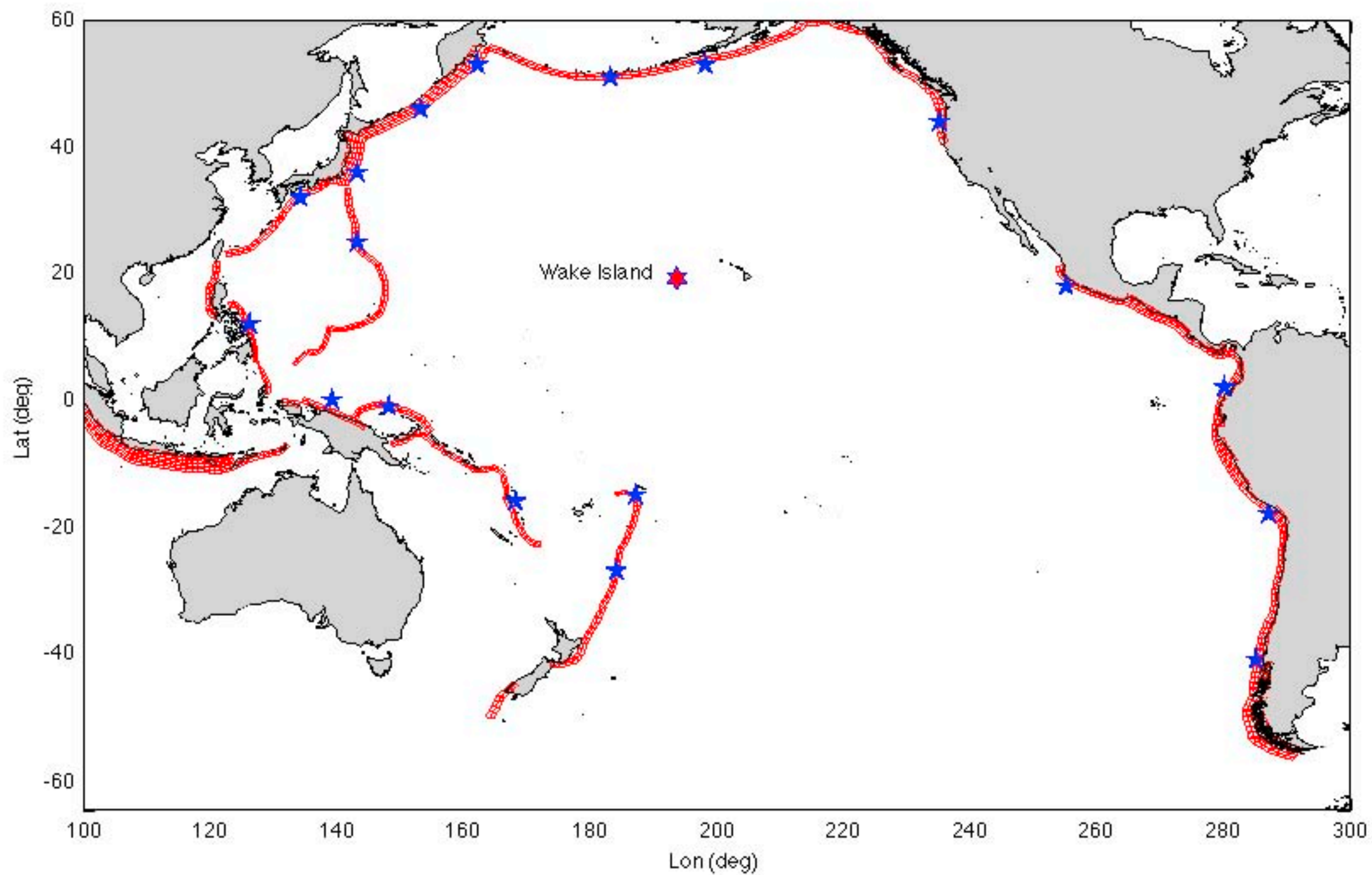




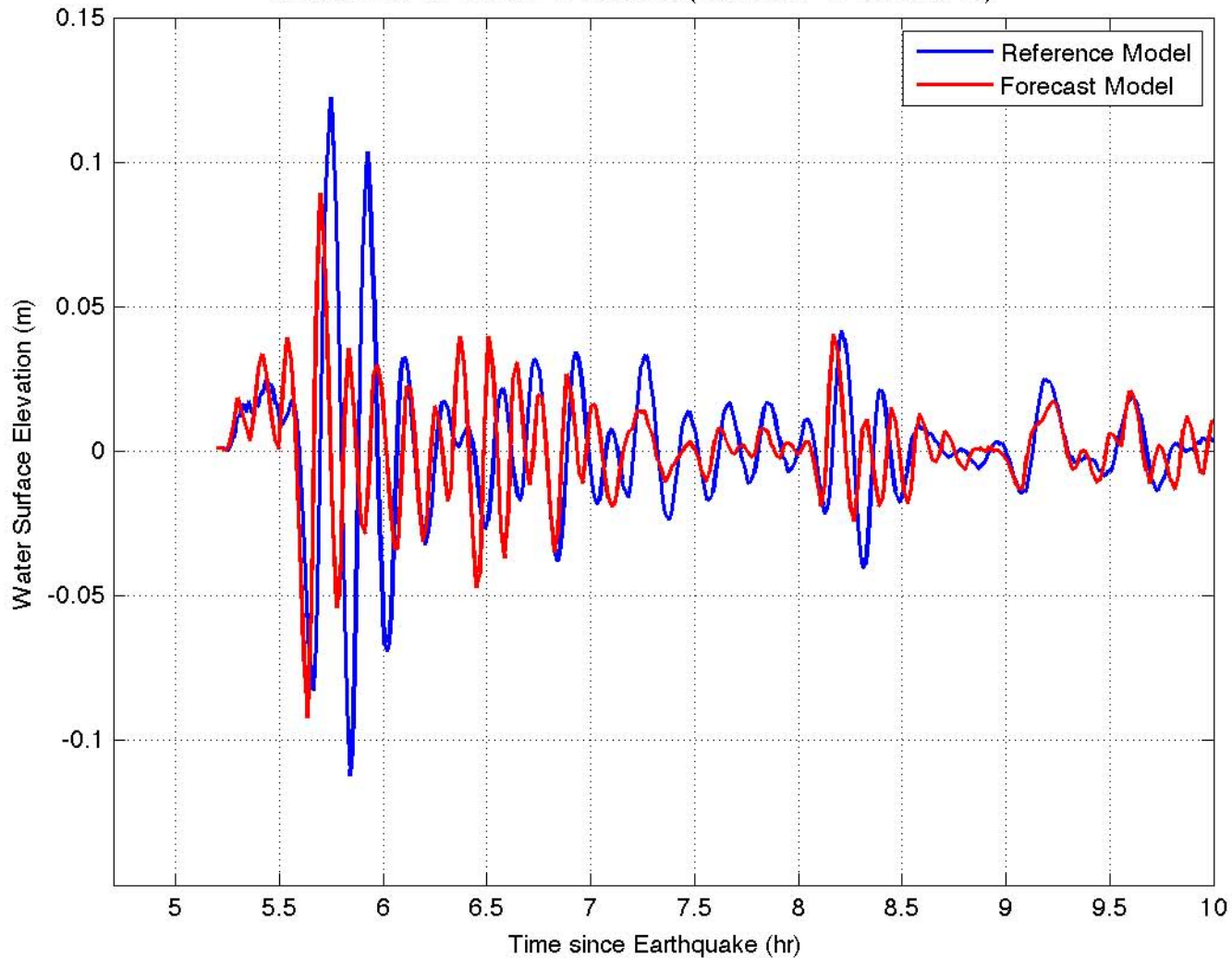




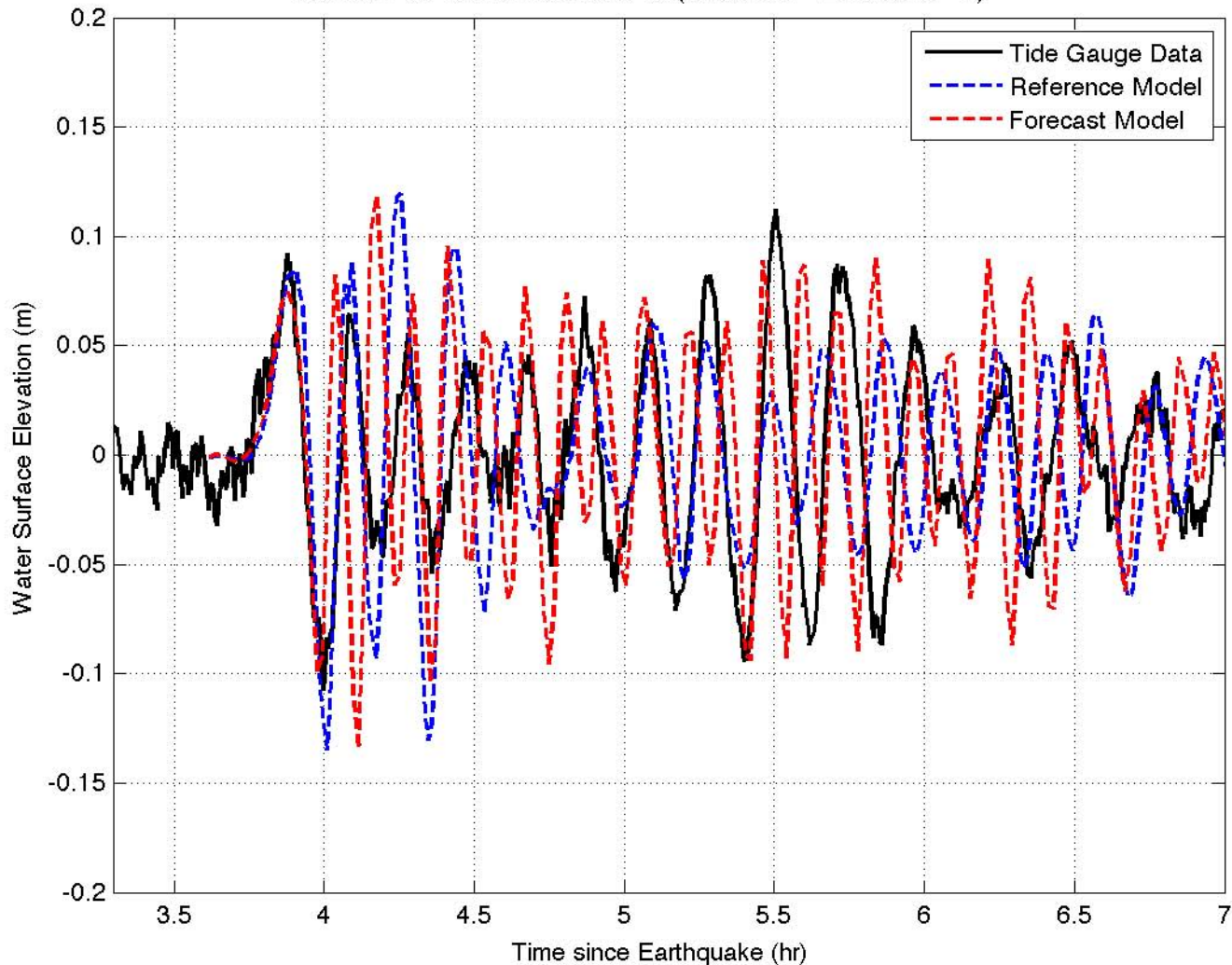




1946 Unimak Is. Tsunami at Wake Is. ( $166.6175^{\circ}$  E  $19.2910^{\circ}$  N)

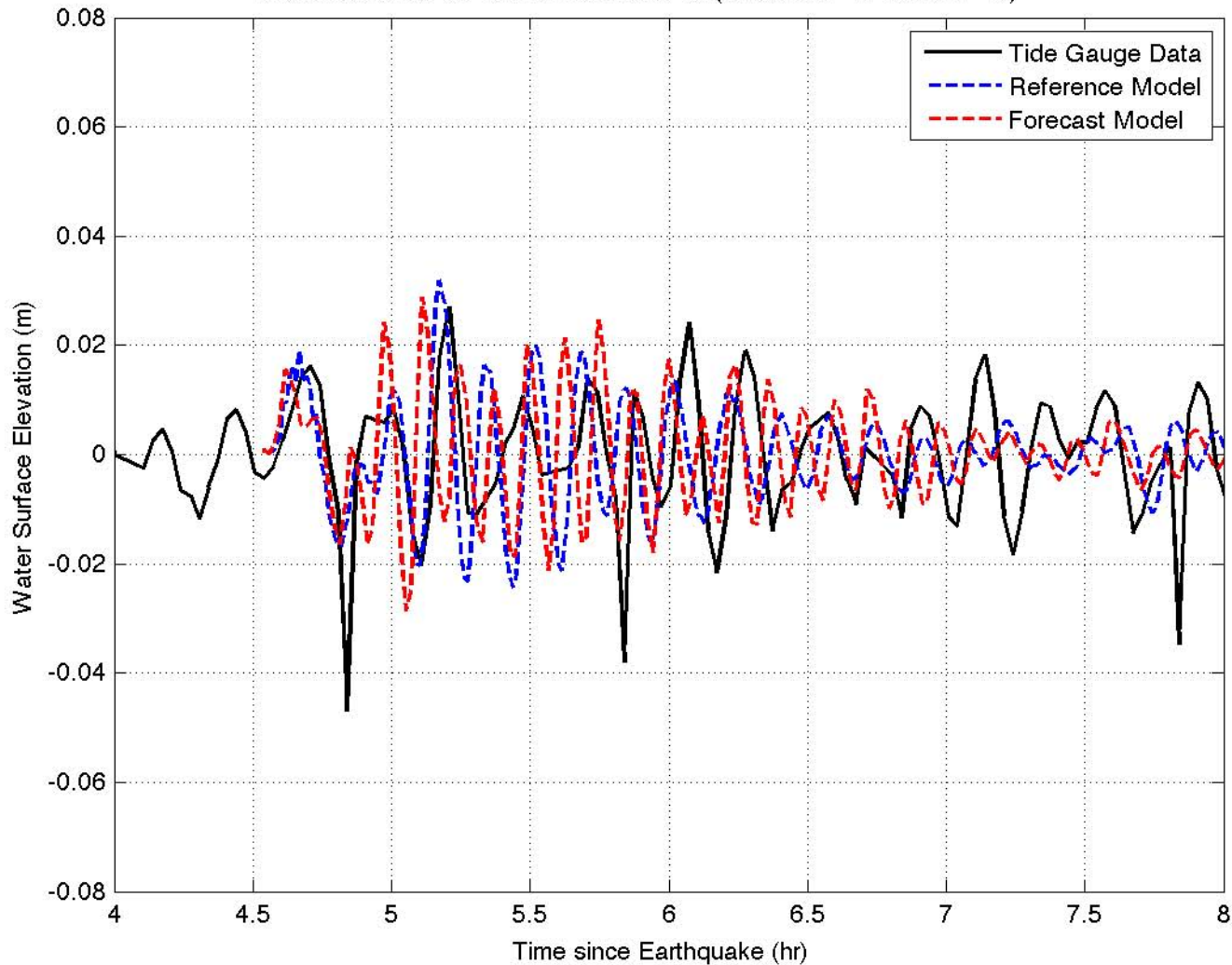


1994 Kuril Is. Tsunami at Wake Is. ( $166.6175^{\circ}$  E  $19.2910^{\circ}$  N)

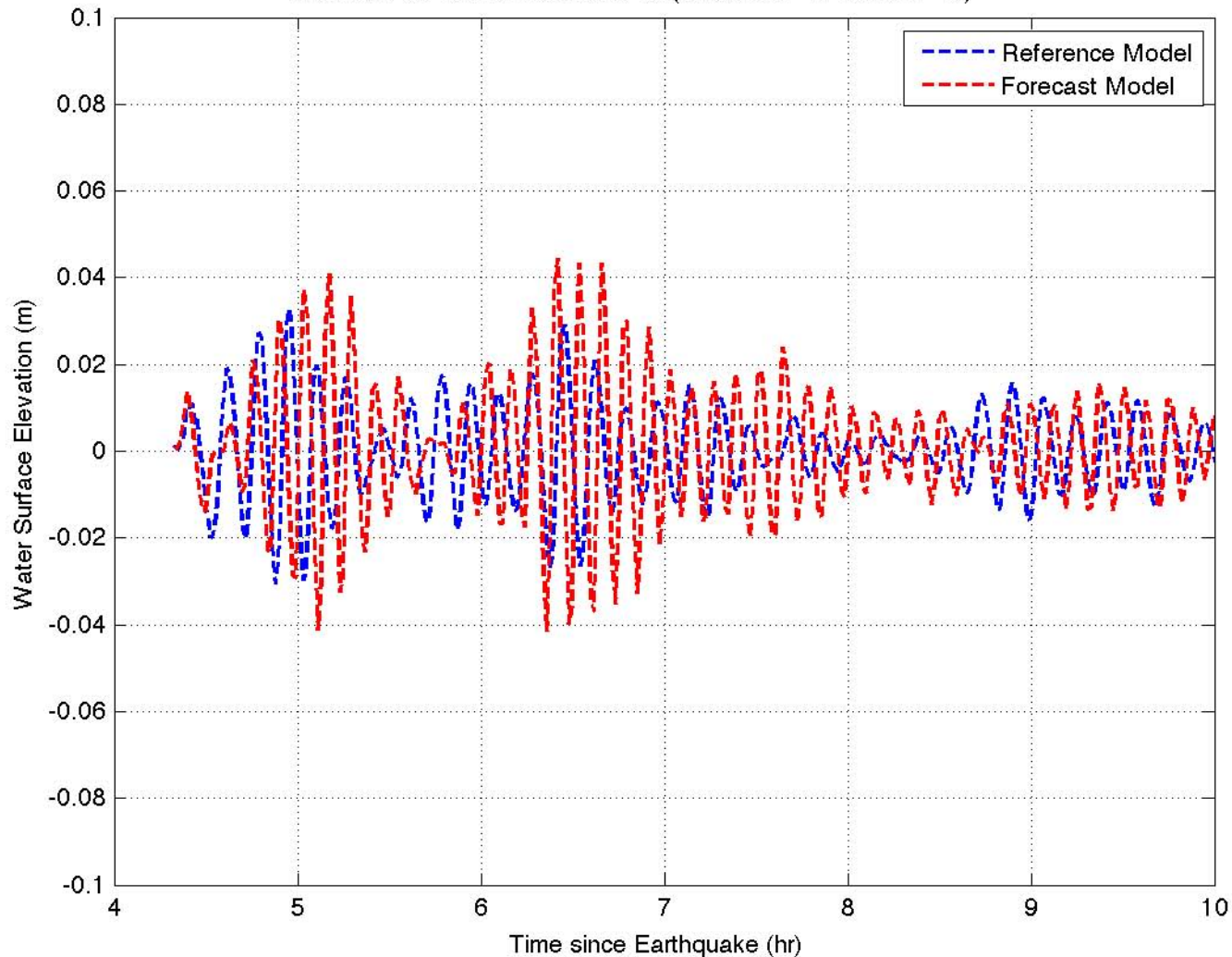




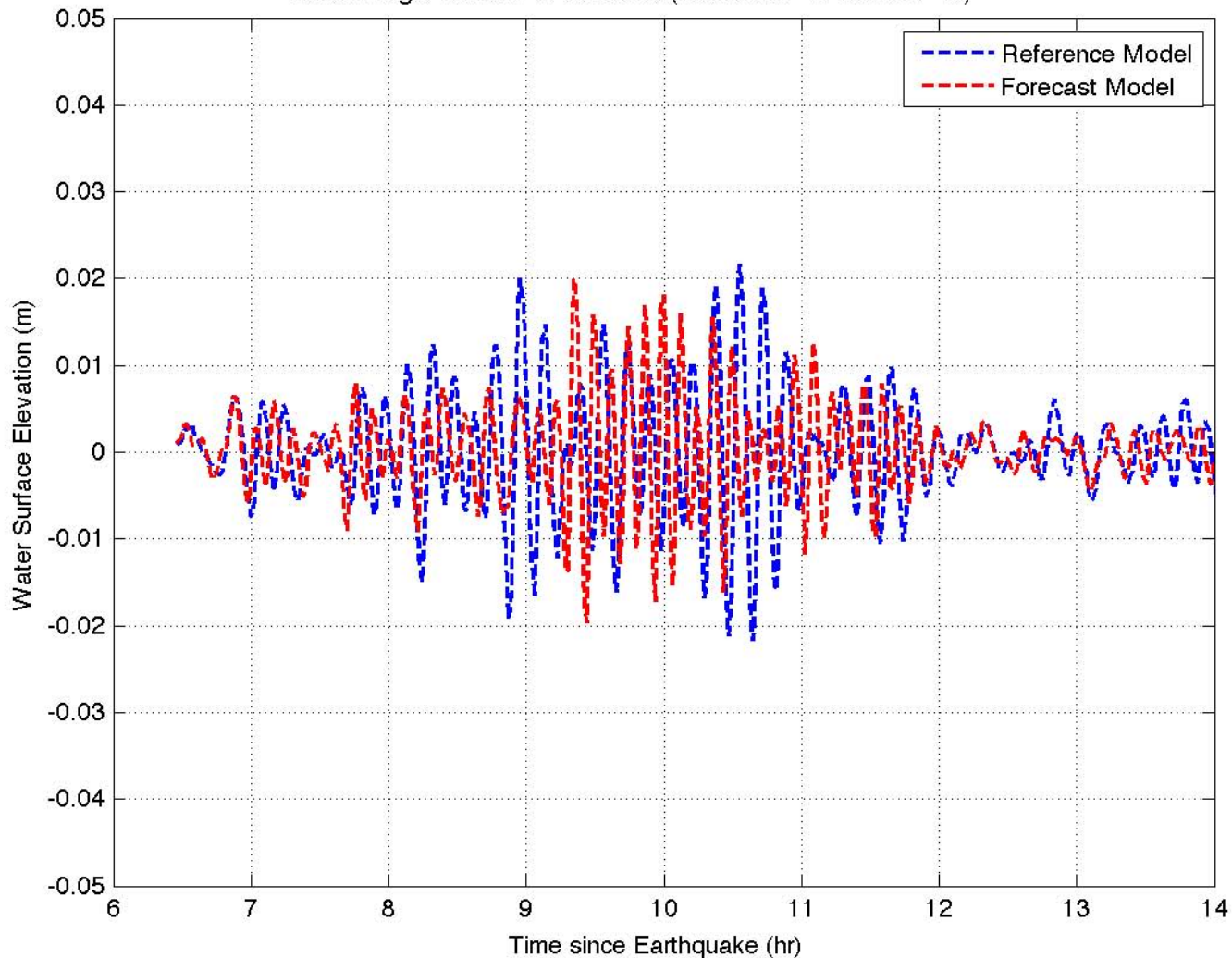
1996 Andreanov Is. Tsunami at Wake Is. ( $166.6175^{\circ}$  E  $19.2910^{\circ}$  N)



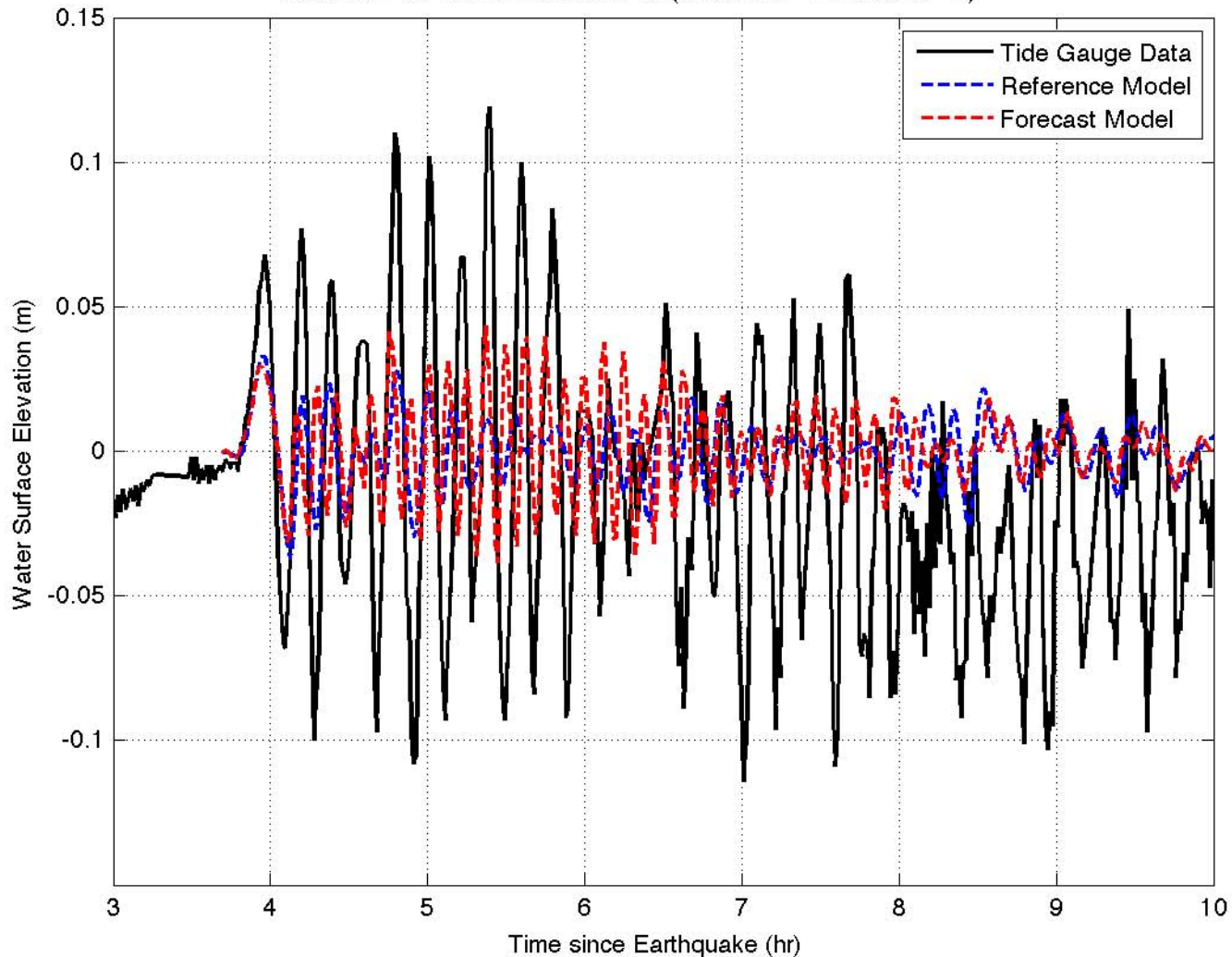
2003 Rat Is. Tsunami at Wake Is. ( $166.6175^{\circ}$  E  $19.2910^{\circ}$  N)



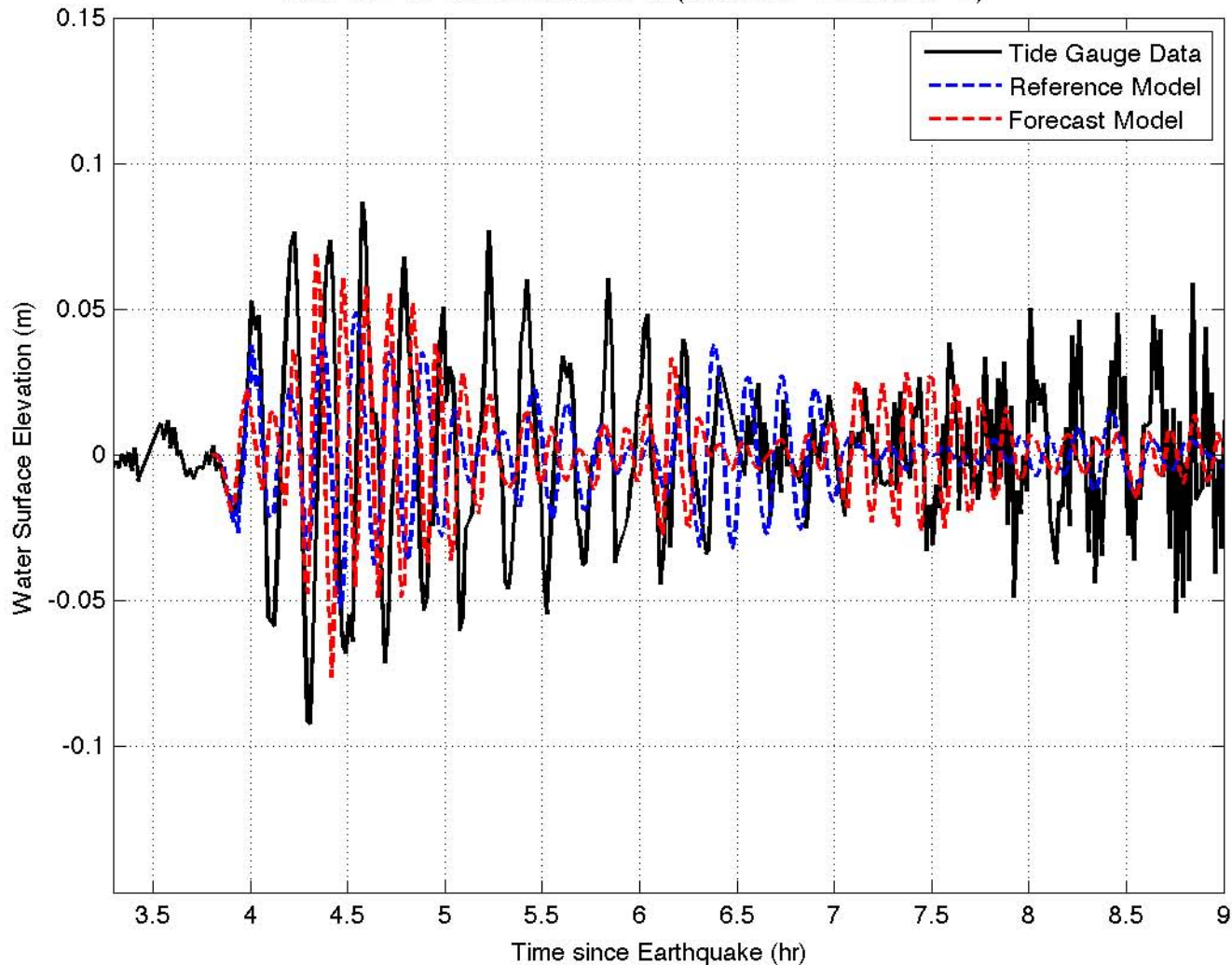
2006 Tonga Tsunami at Wake Is. ( $166.6175^{\circ}$  E  $19.2910^{\circ}$  N)



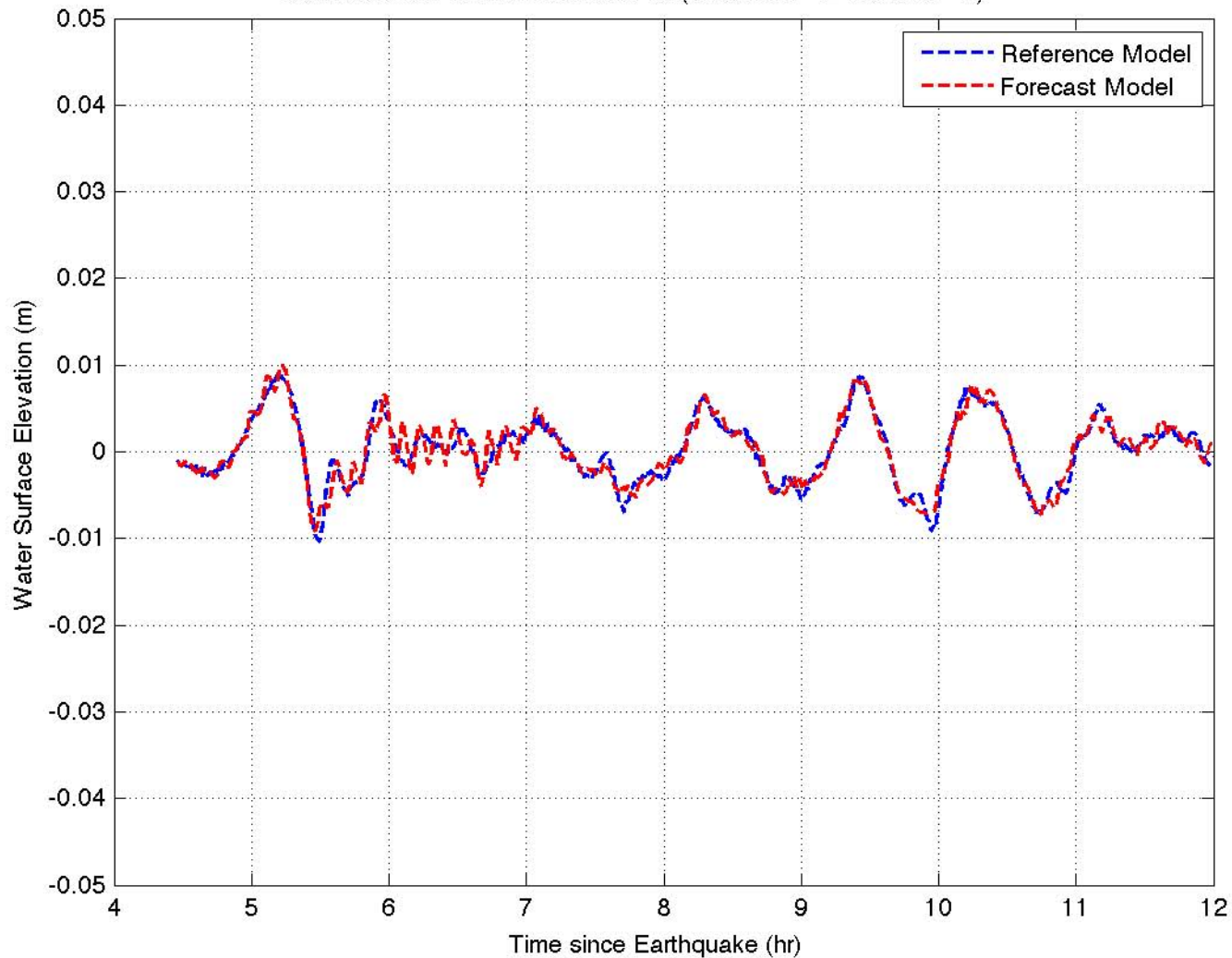
2006 Kuril Is. Tsunami at Wake Is. ( $166.6175^{\circ}$  E  $19.2910^{\circ}$  N)



2007 Kuril Is. Tsunami at Wake Is. ( $166.6175^{\circ}$  E  $19.2910^{\circ}$  N)

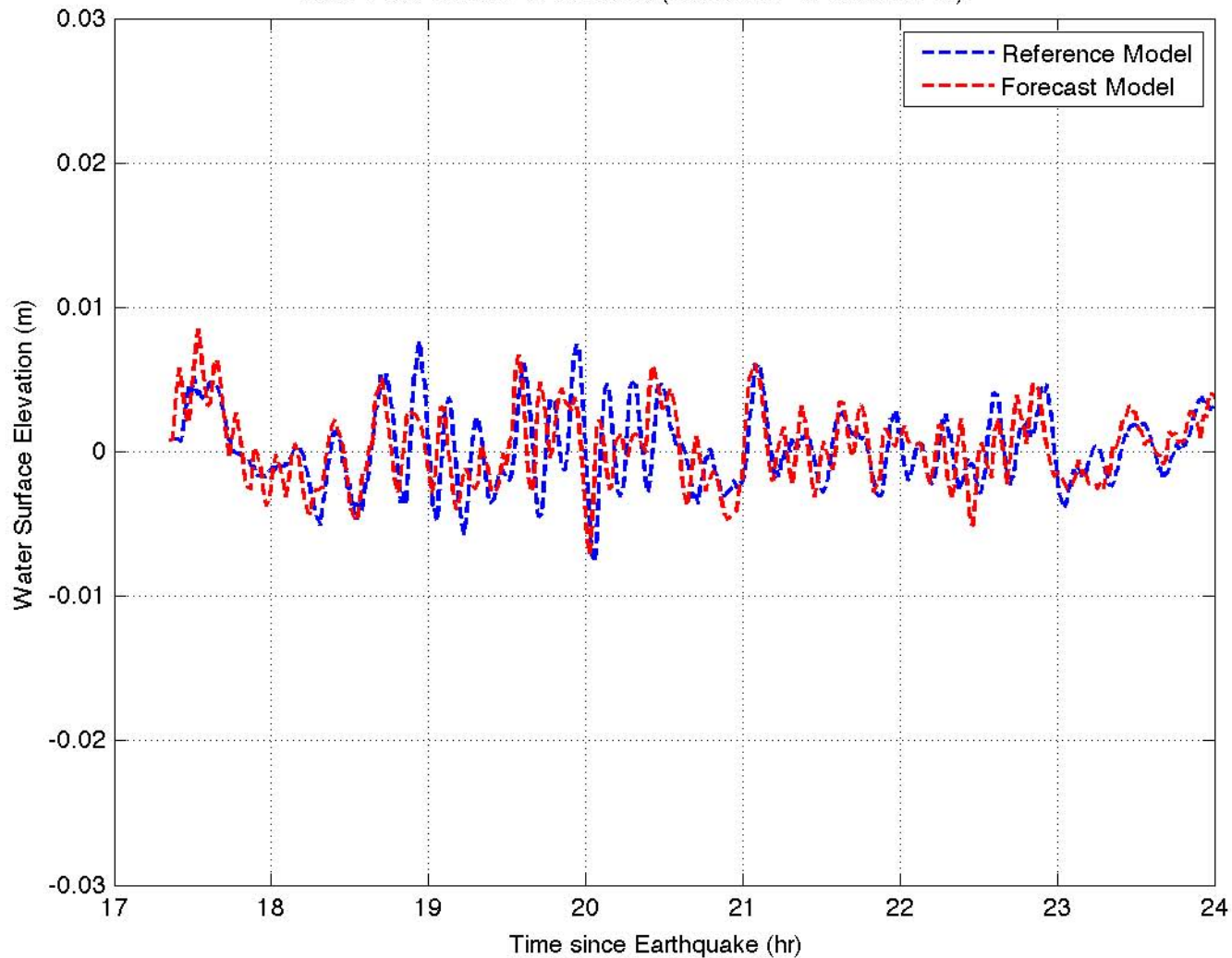


2007 Solomon Tsunami at Wake Is. ( $166.6175^{\circ}$  E  $19.2910^{\circ}$  N)

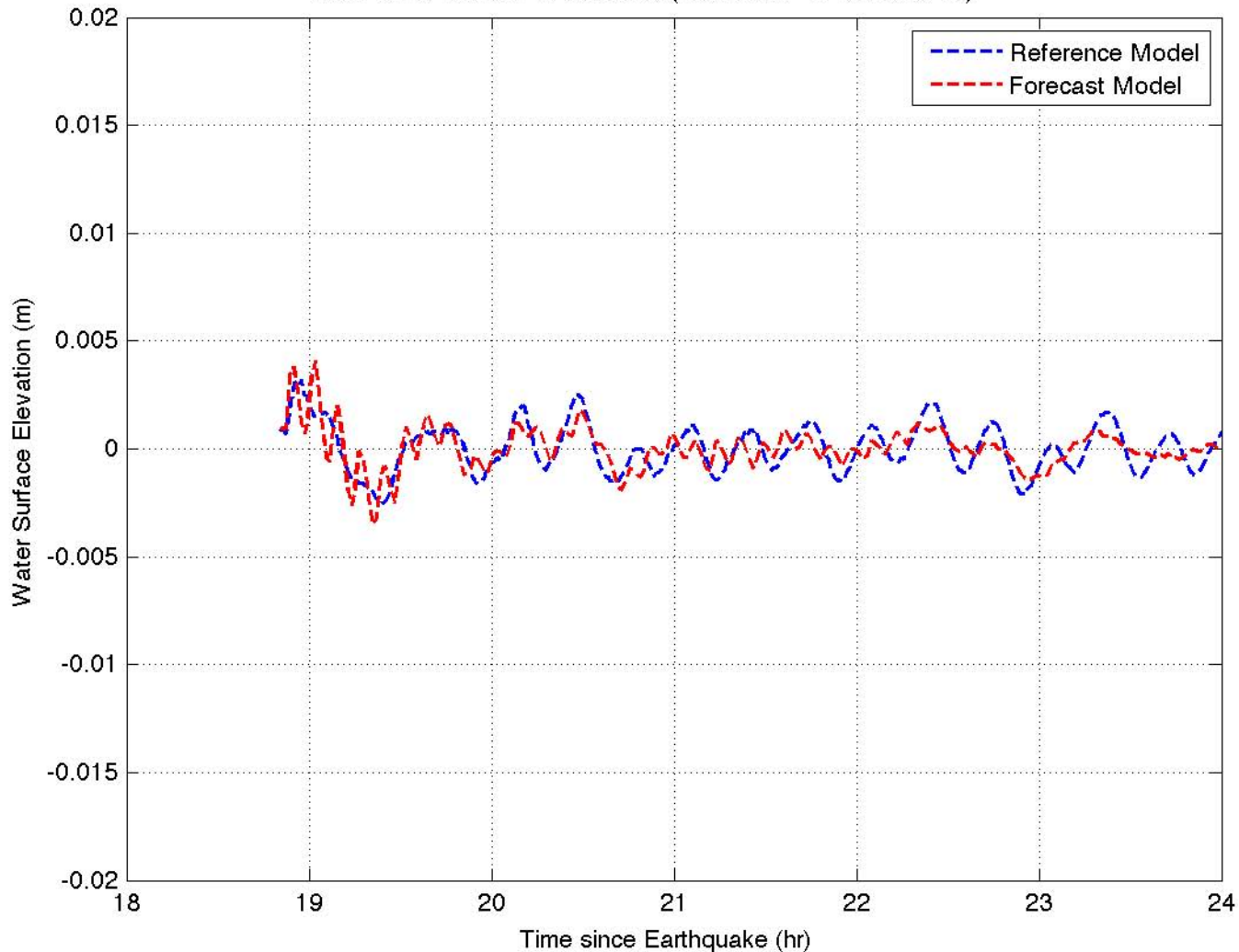




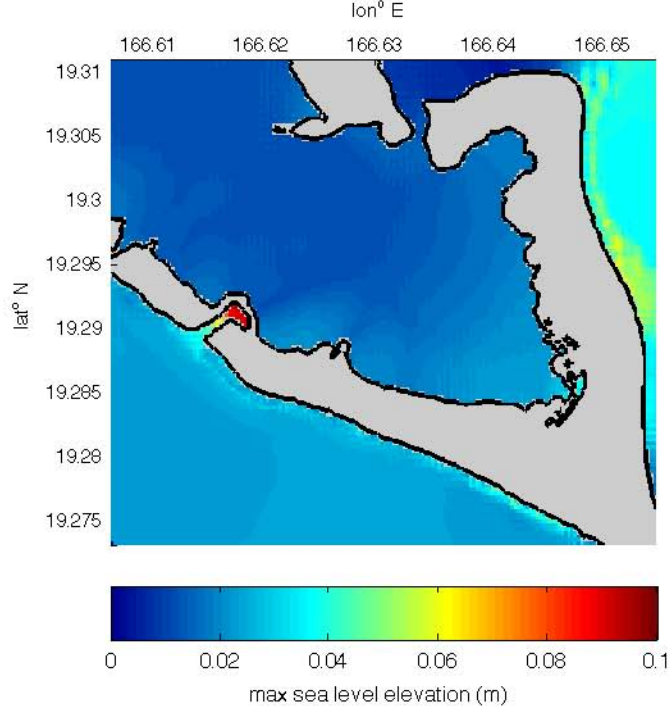
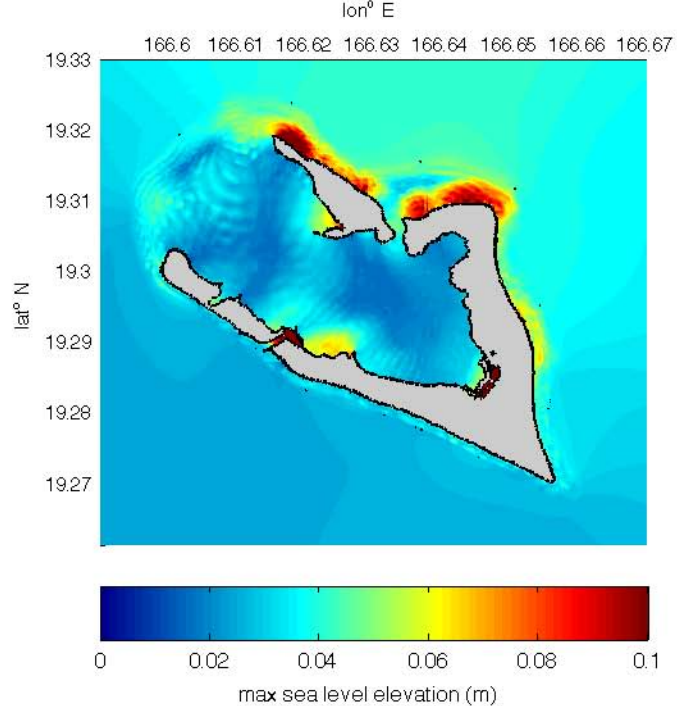
2007 Peru Tsunami at Wake Is. ( $166.6175^{\circ}$  E  $19.2910^{\circ}$  N)

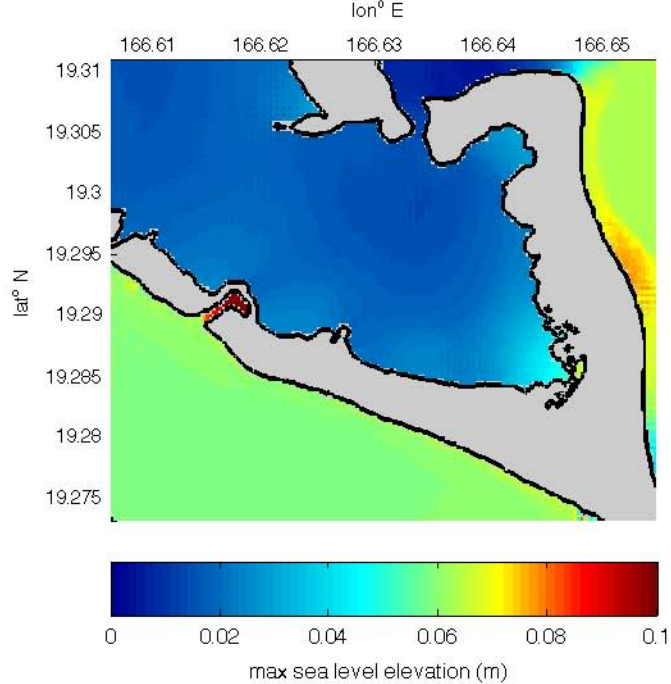
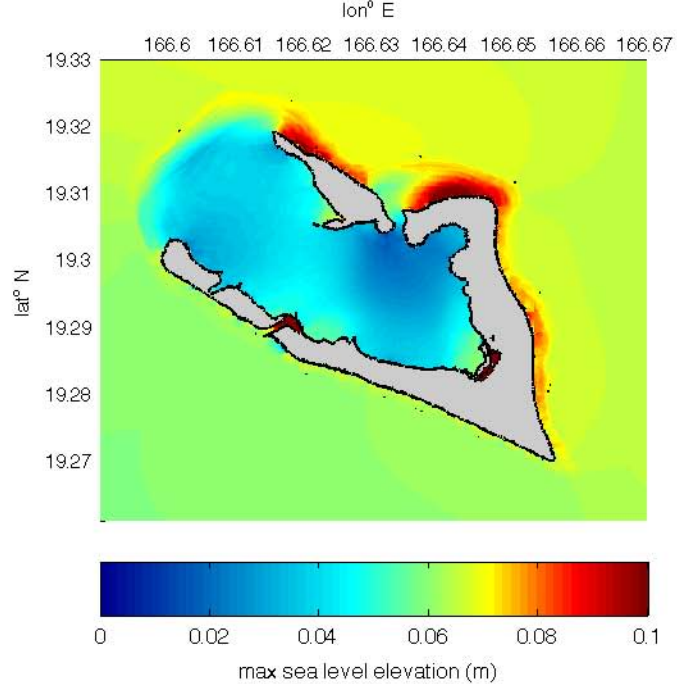


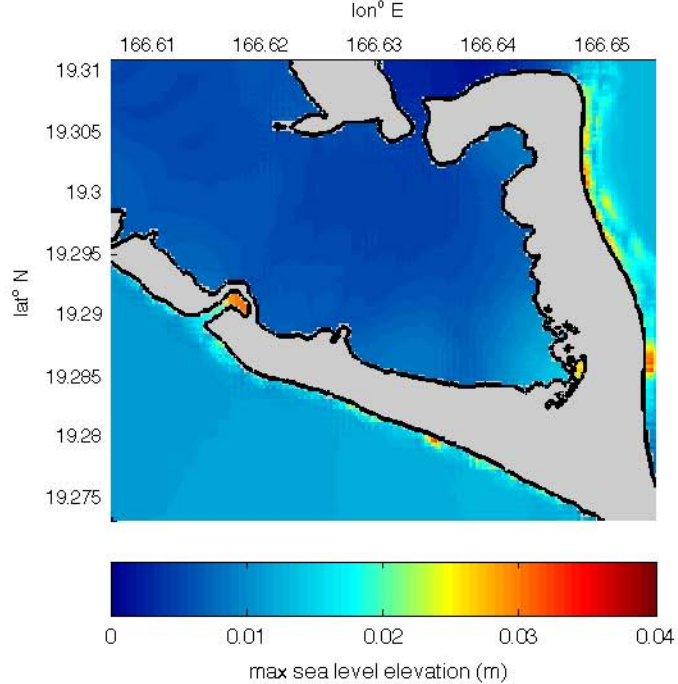
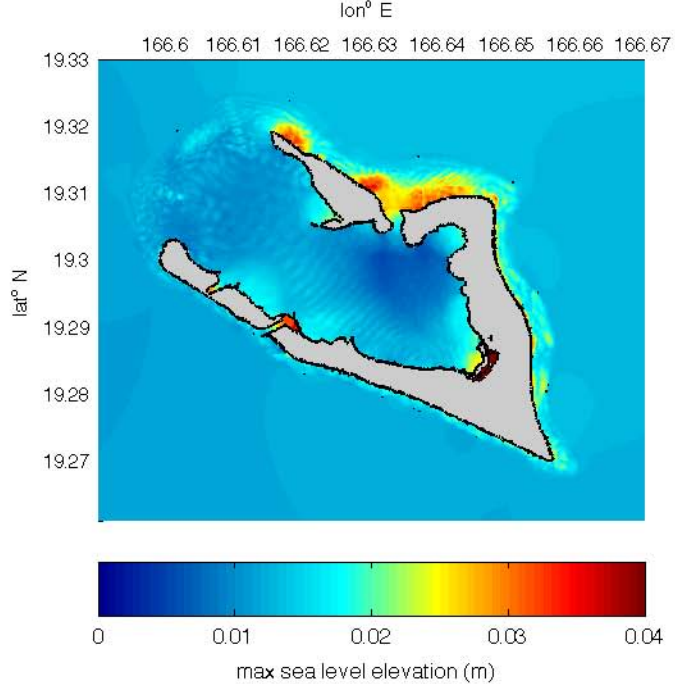
2007 Chile Tsunami at Wake Is. ( $166.6175^{\circ}$  E  $19.2910^{\circ}$  N)

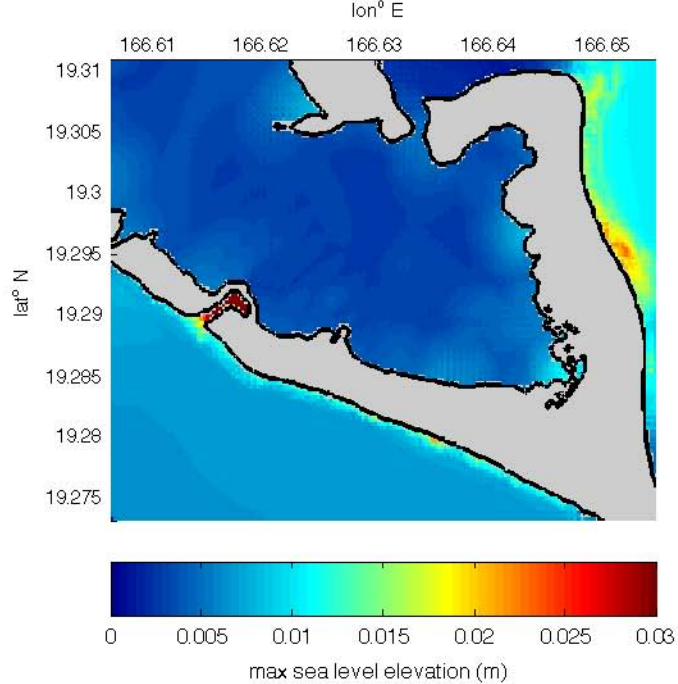
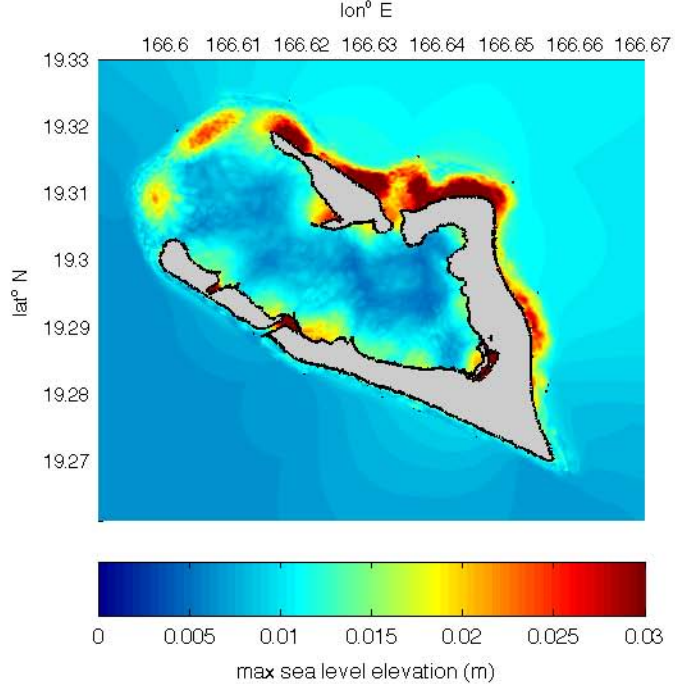


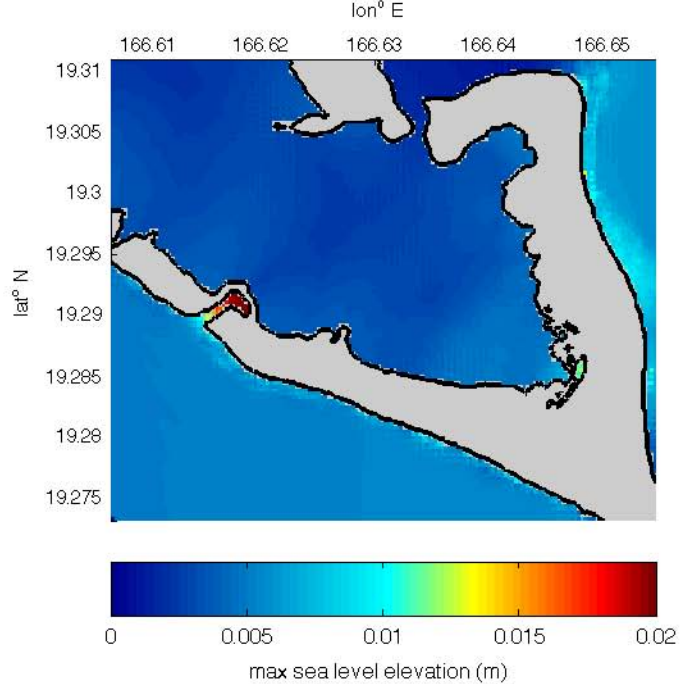
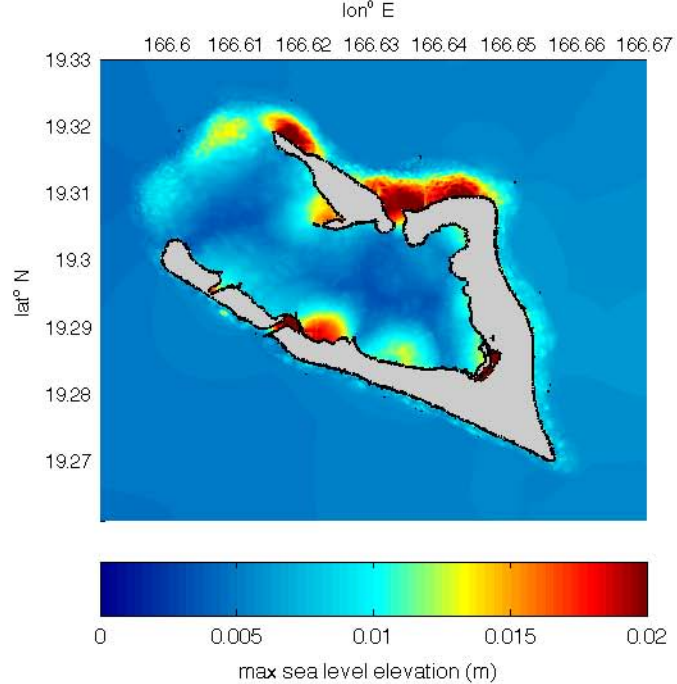


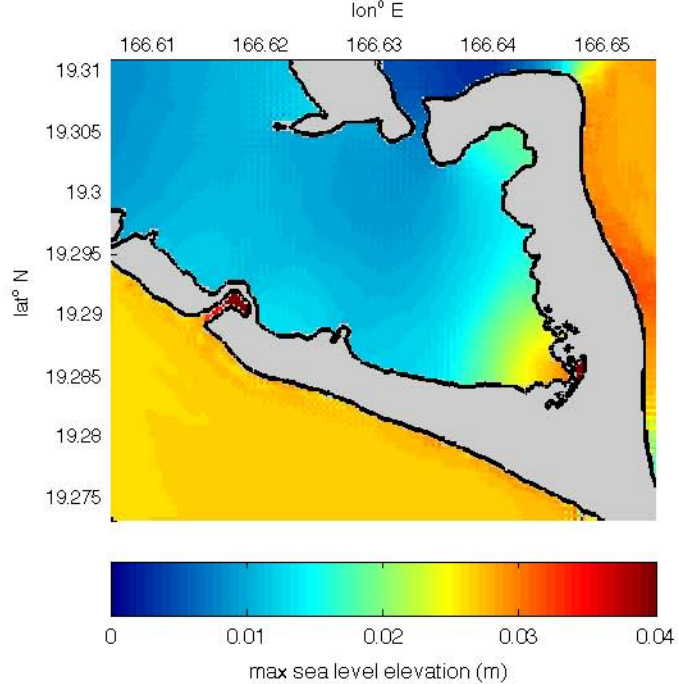
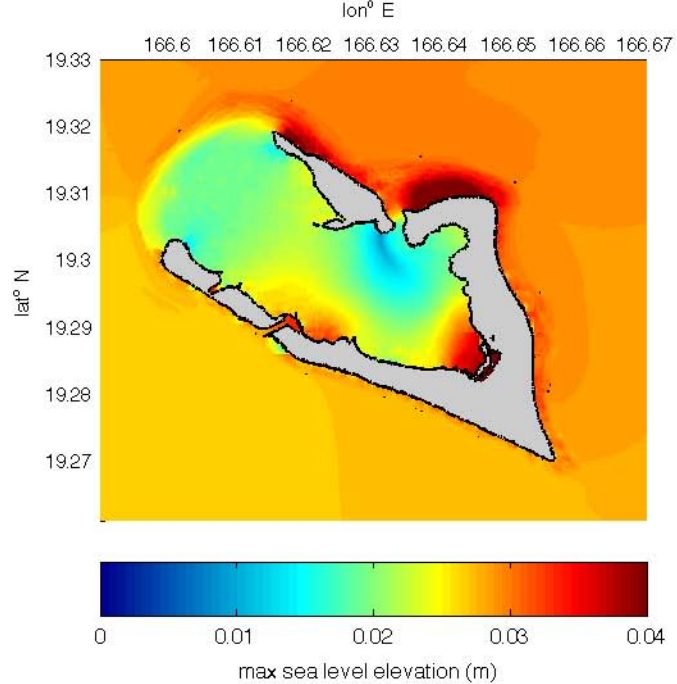


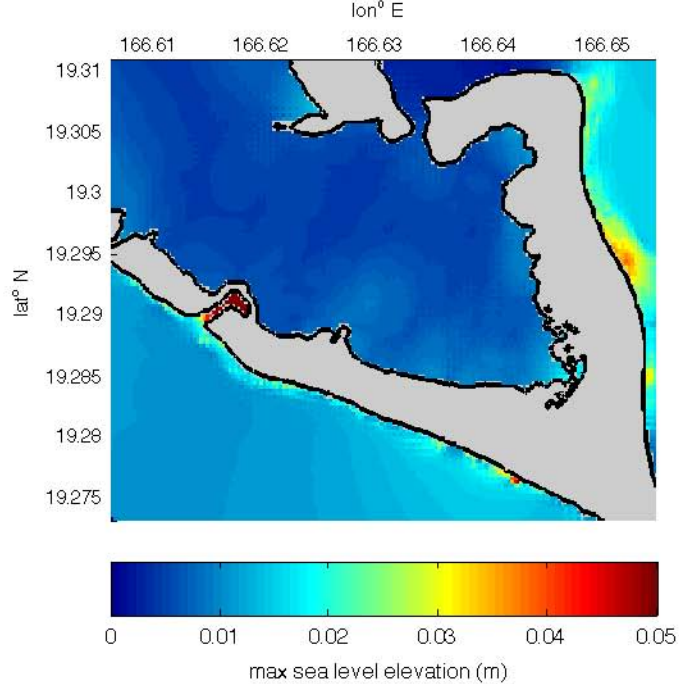
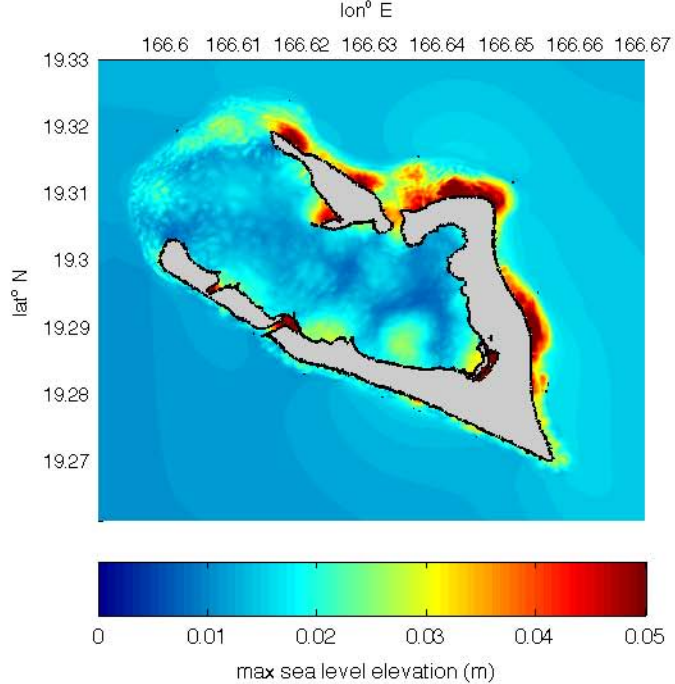




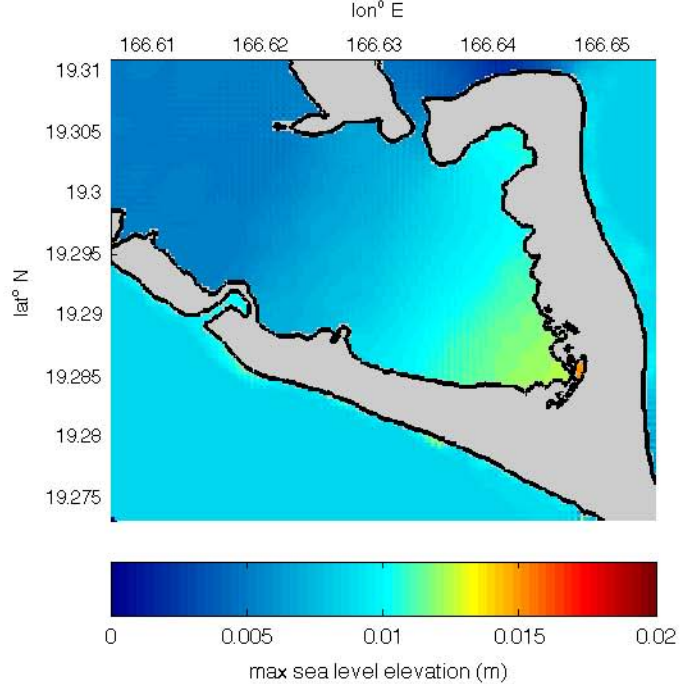
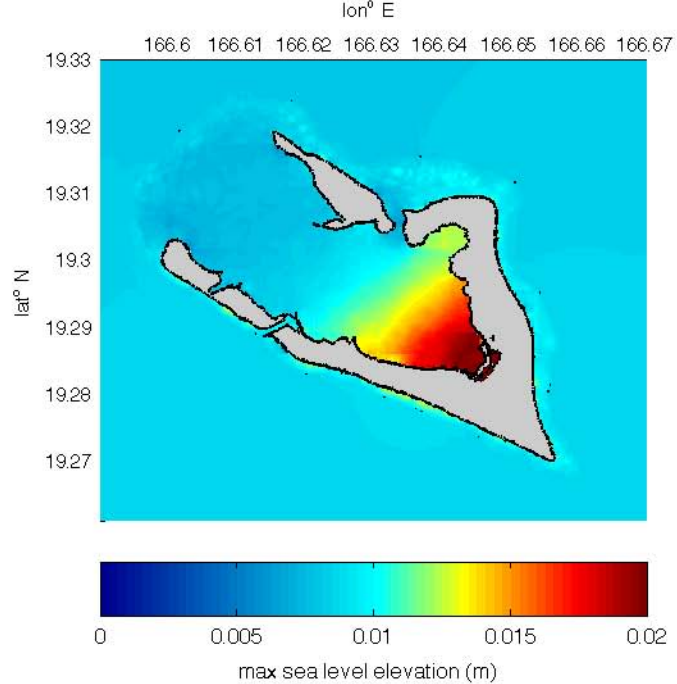




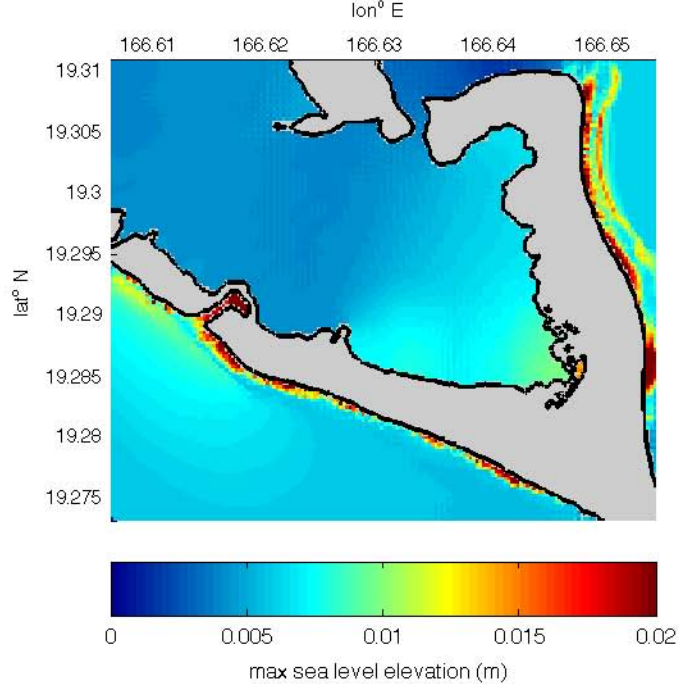
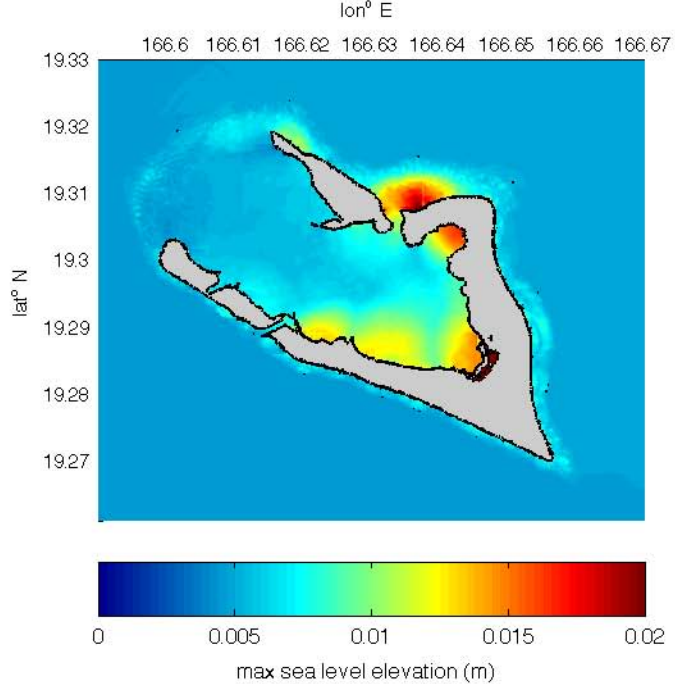


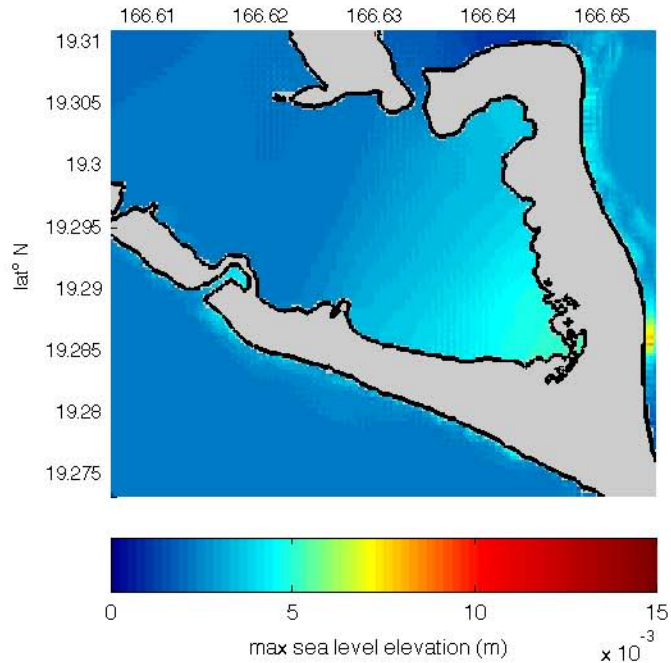
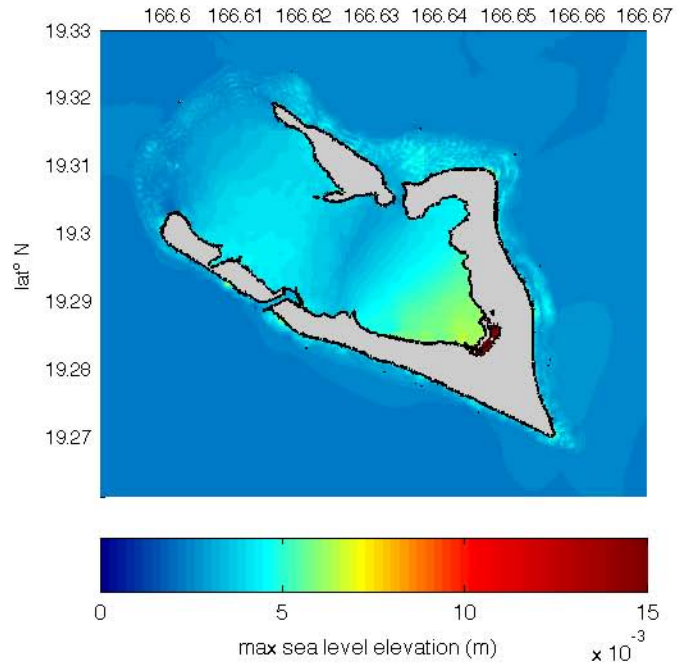


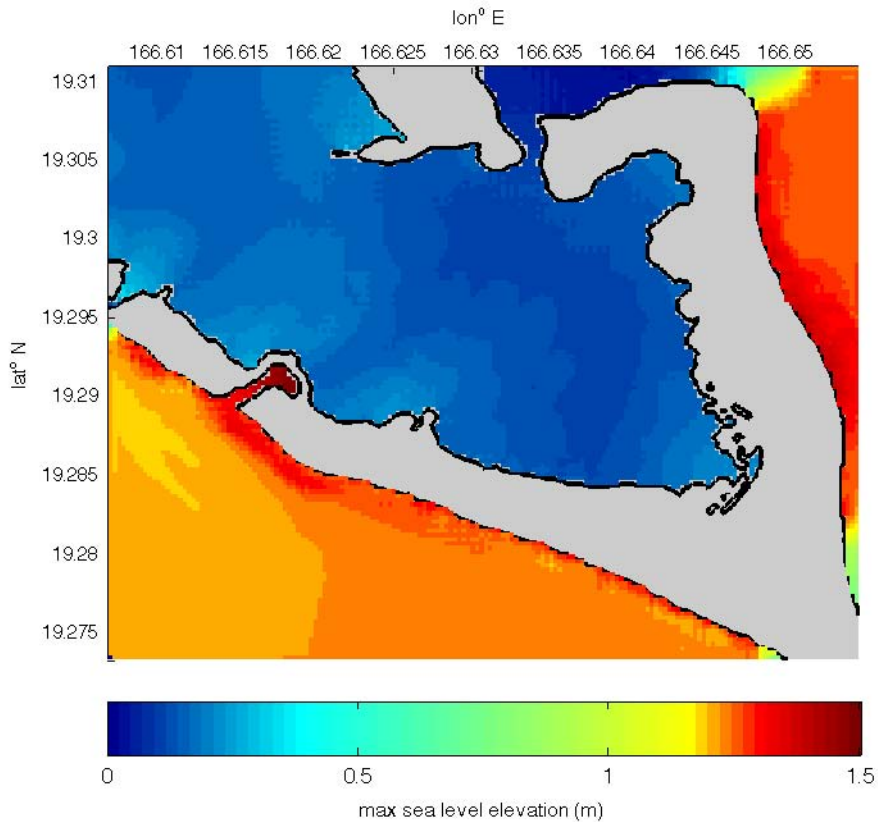


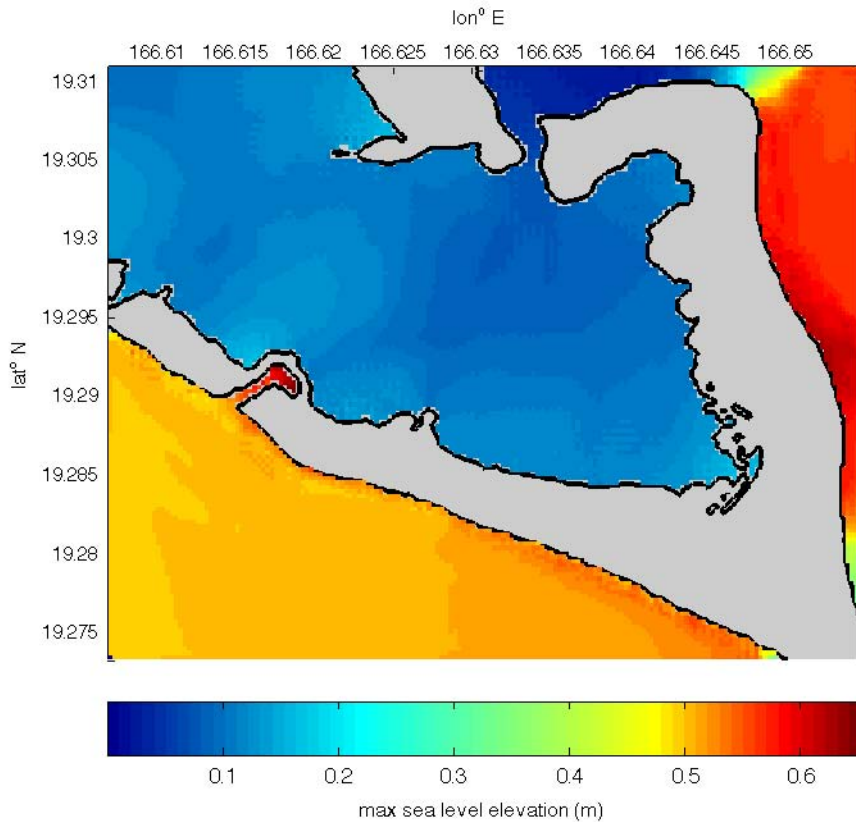


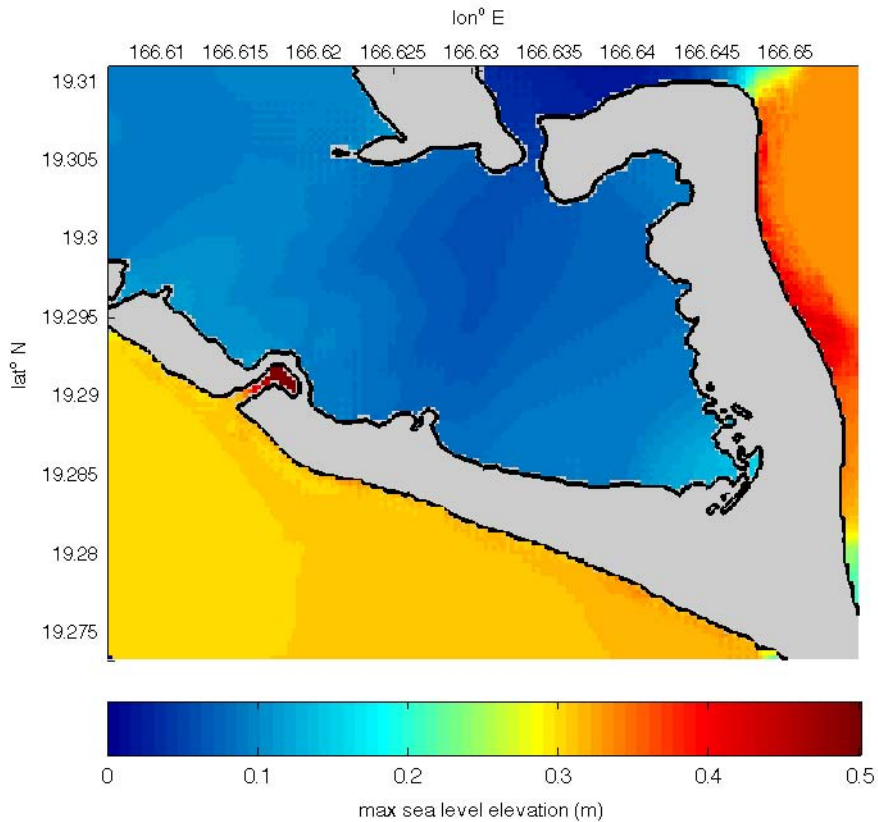


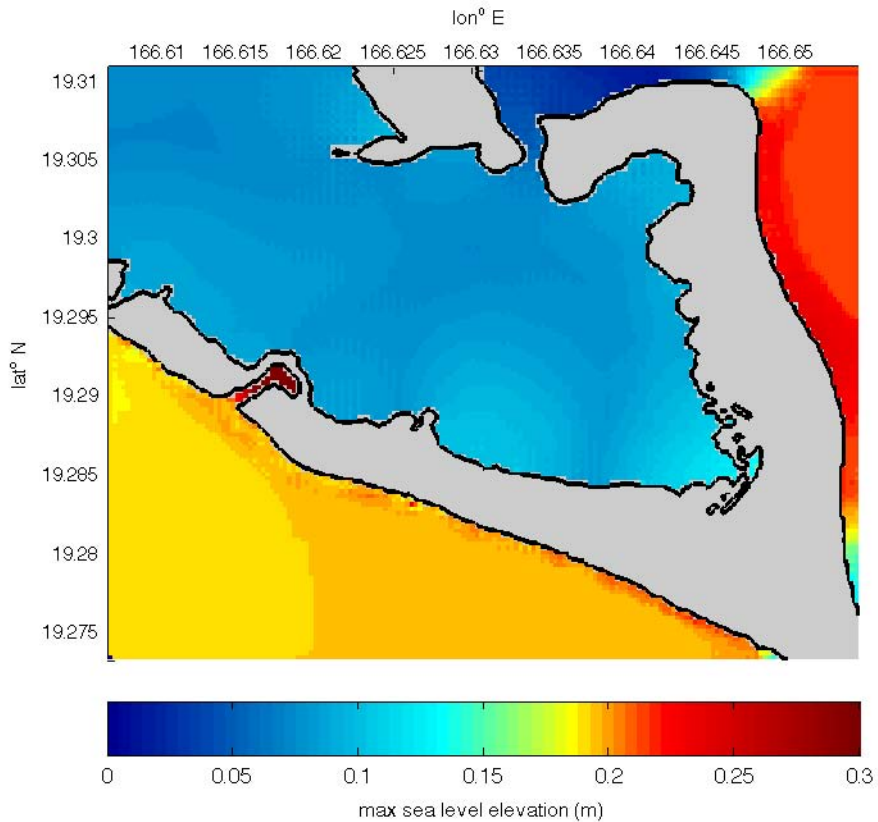


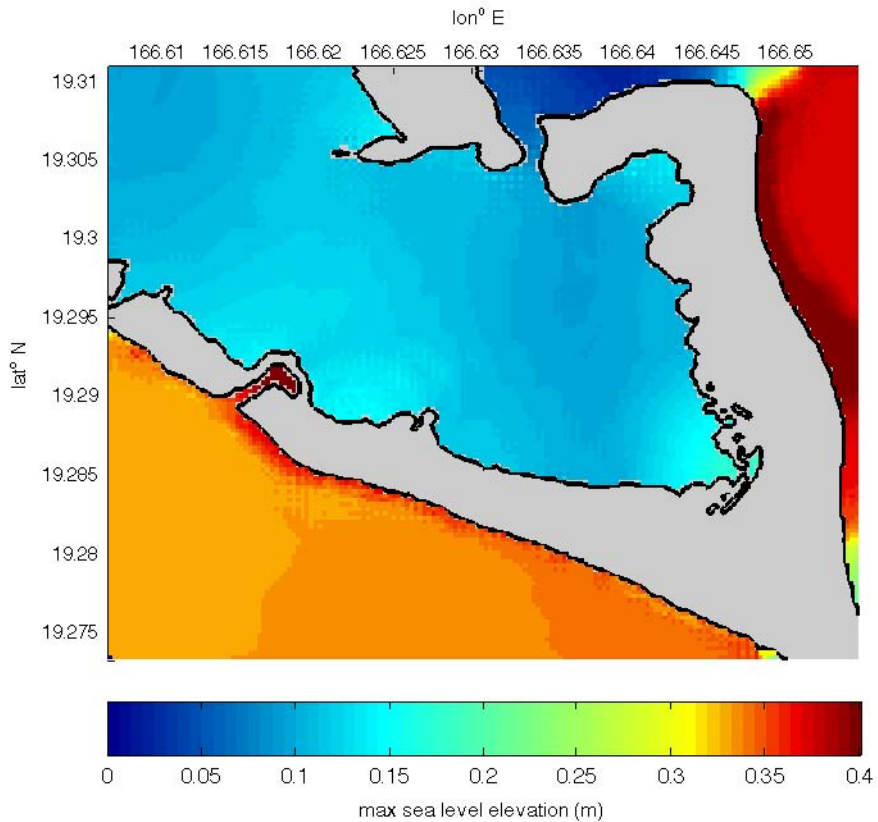


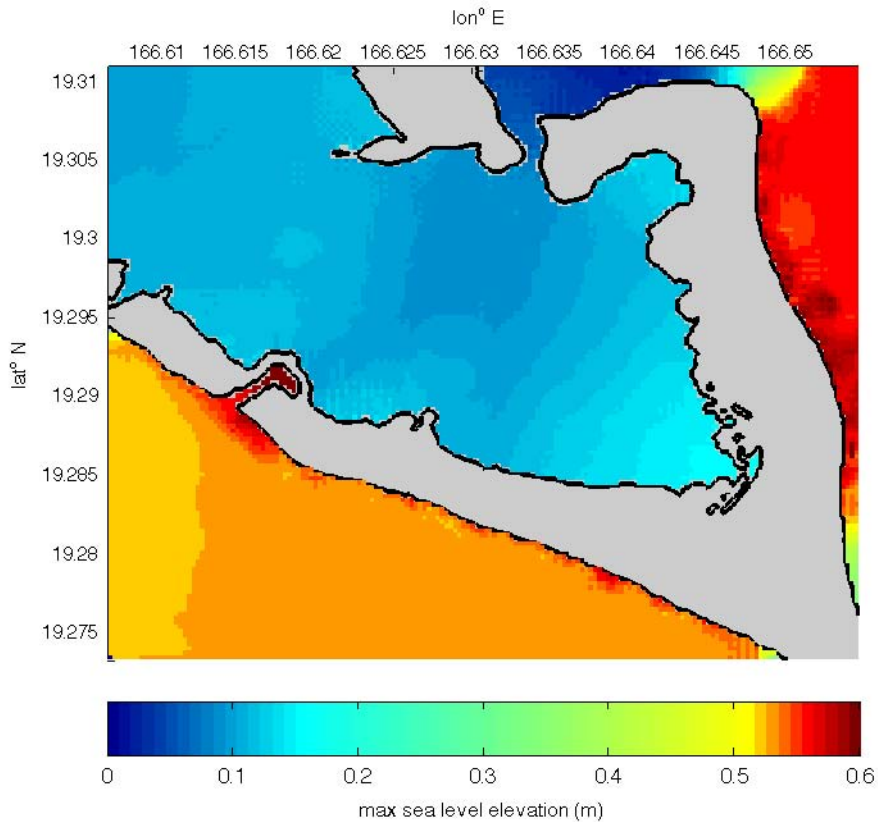




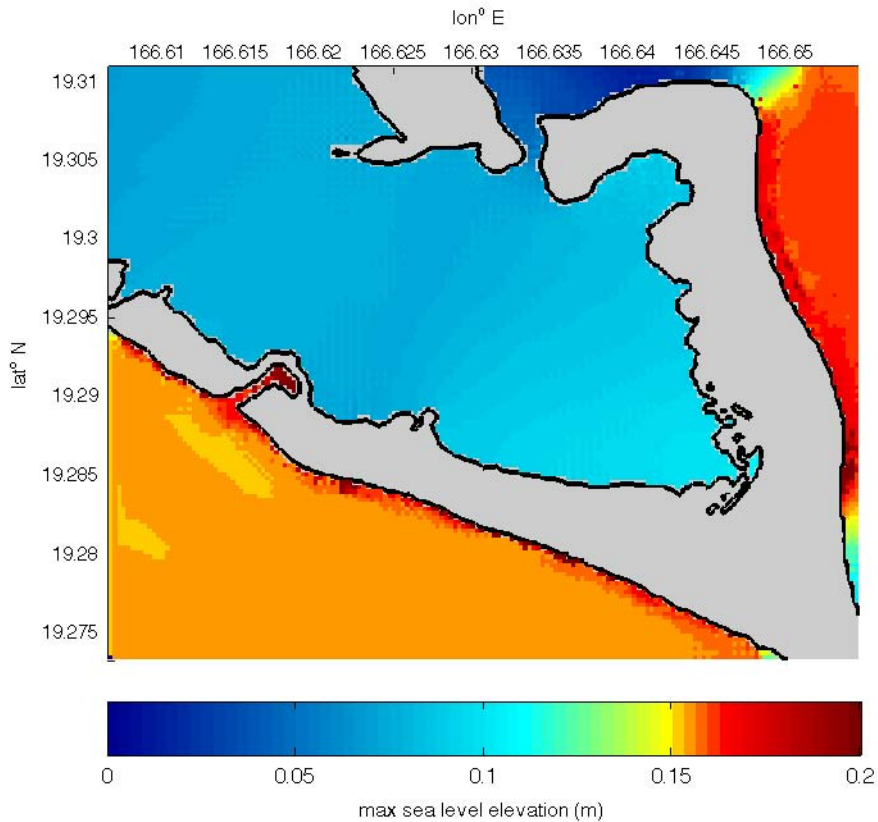


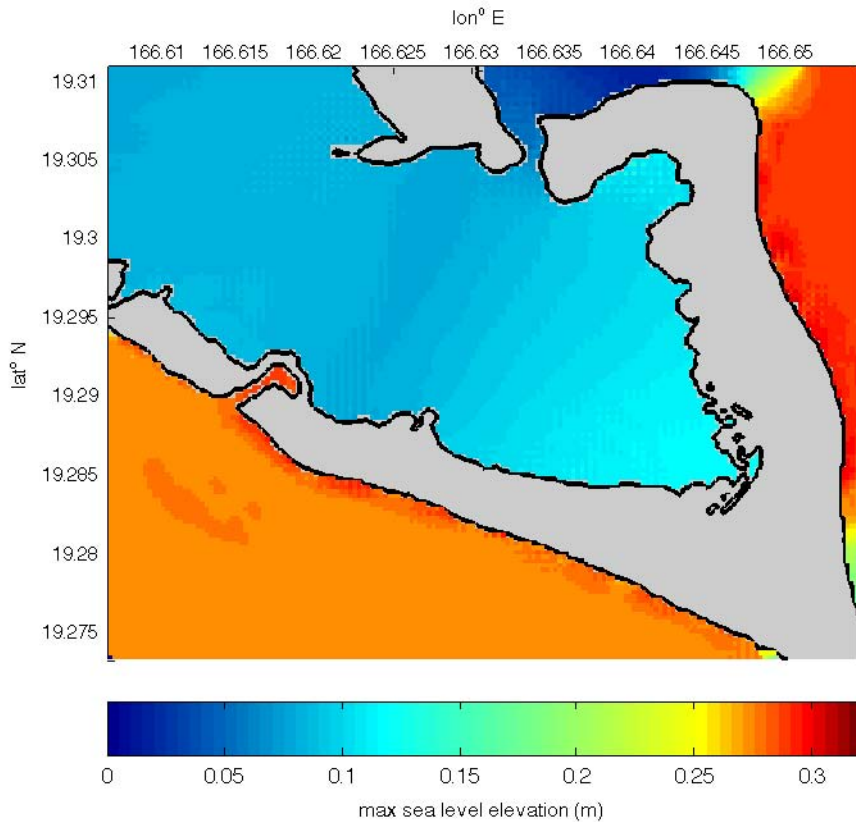


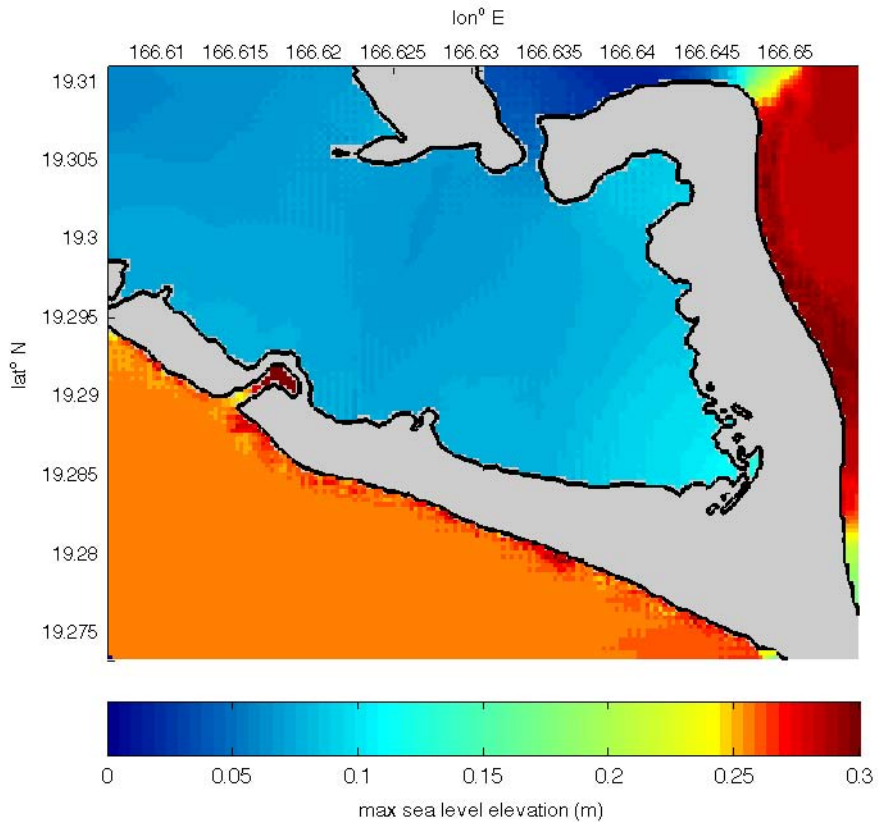


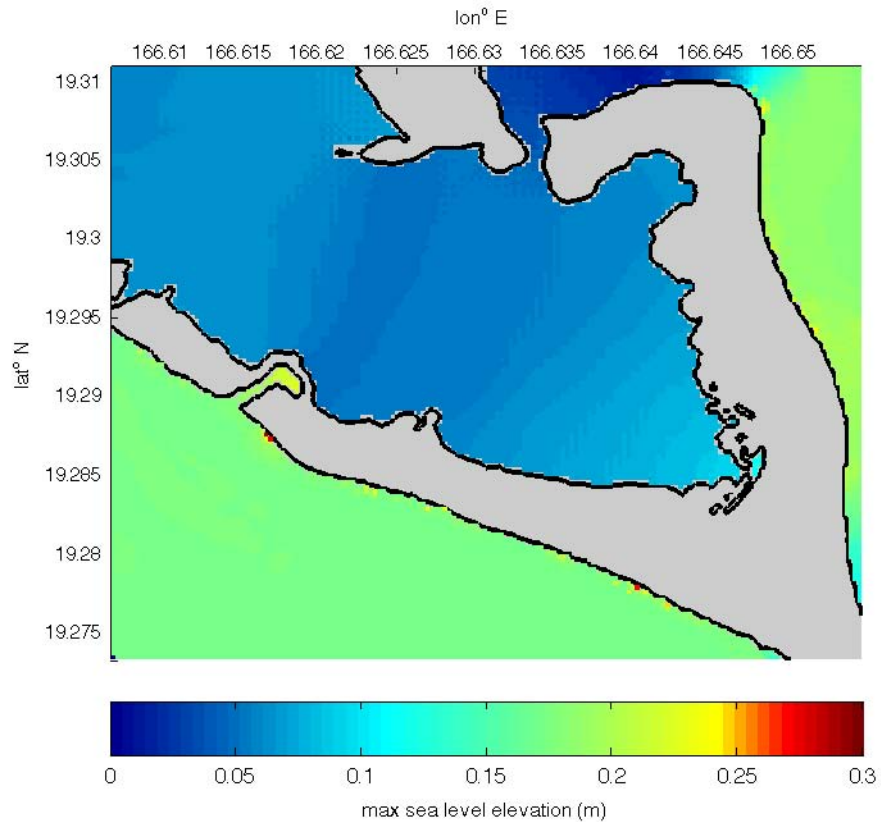


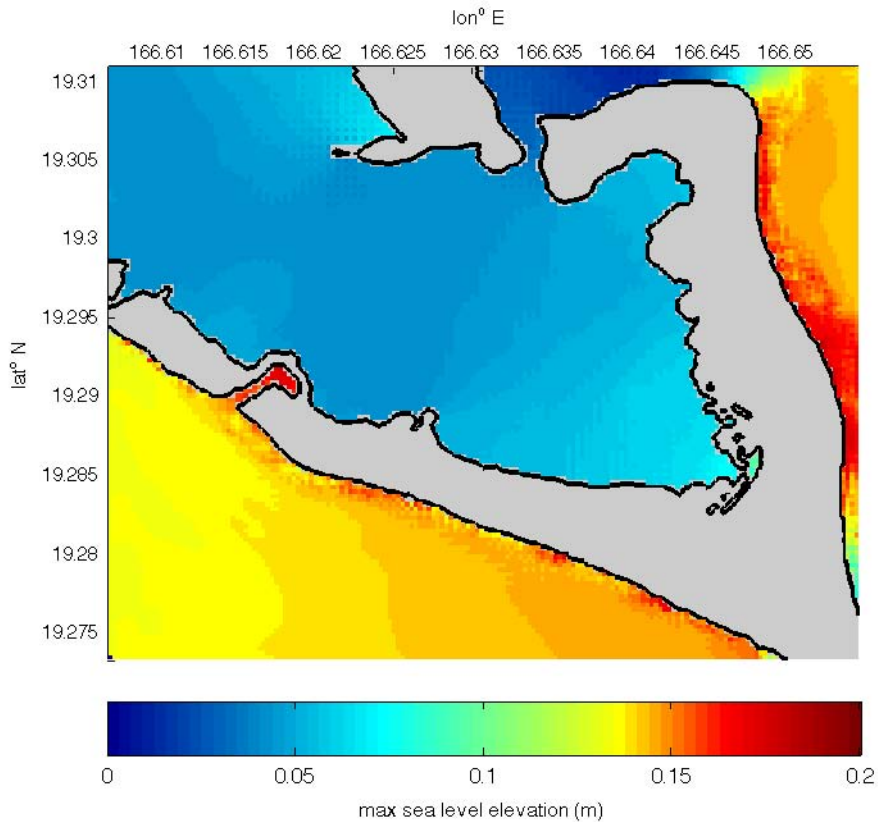


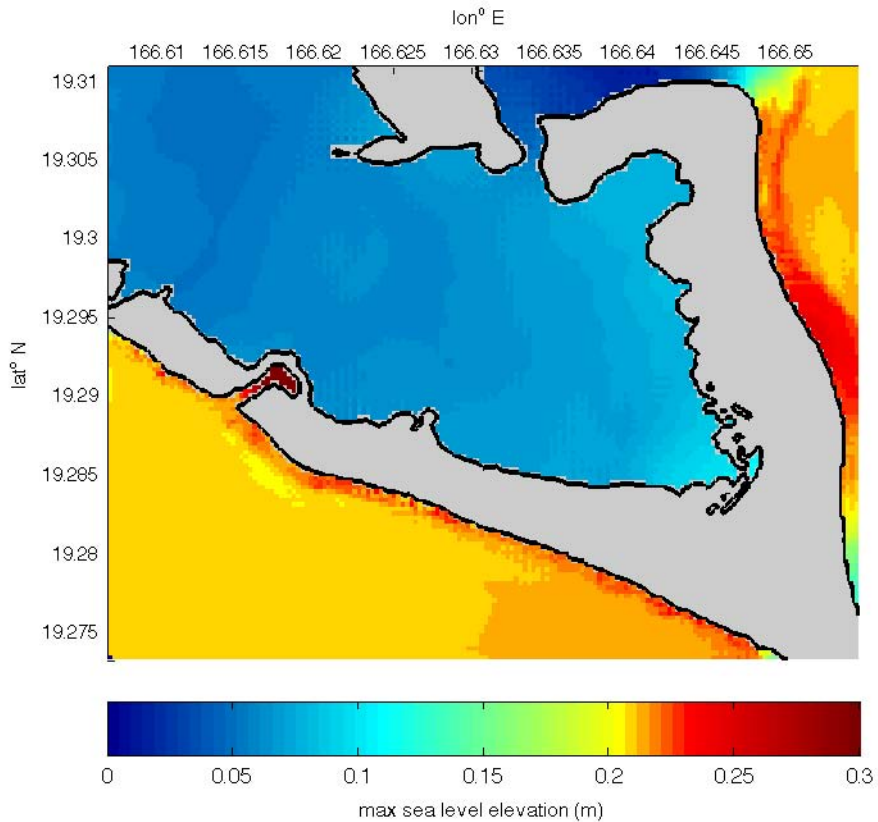


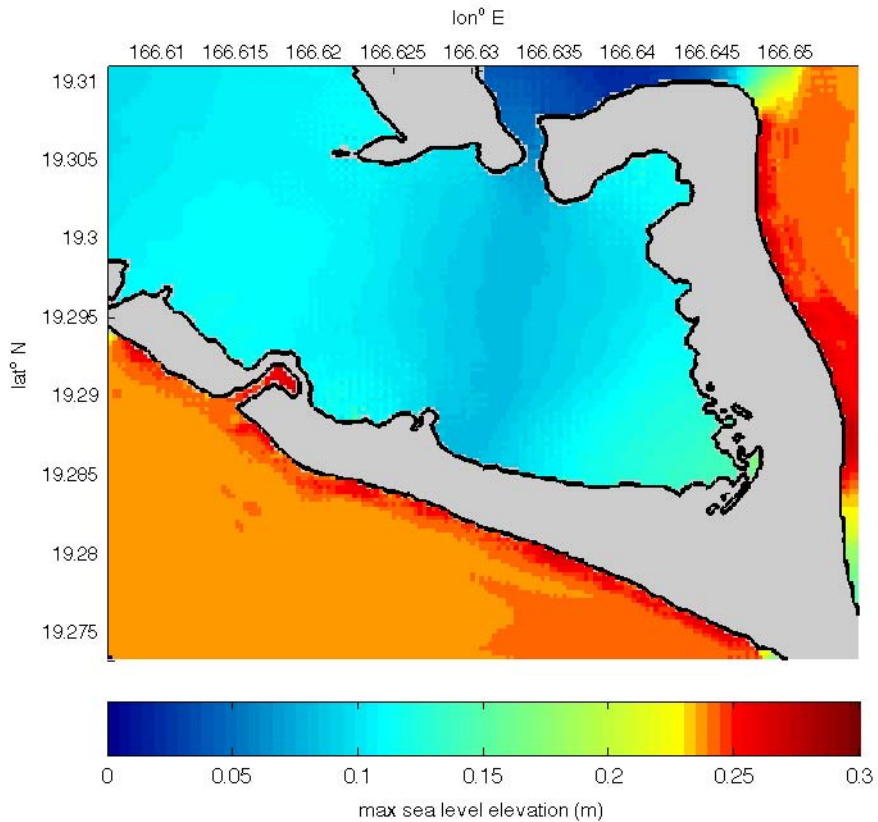


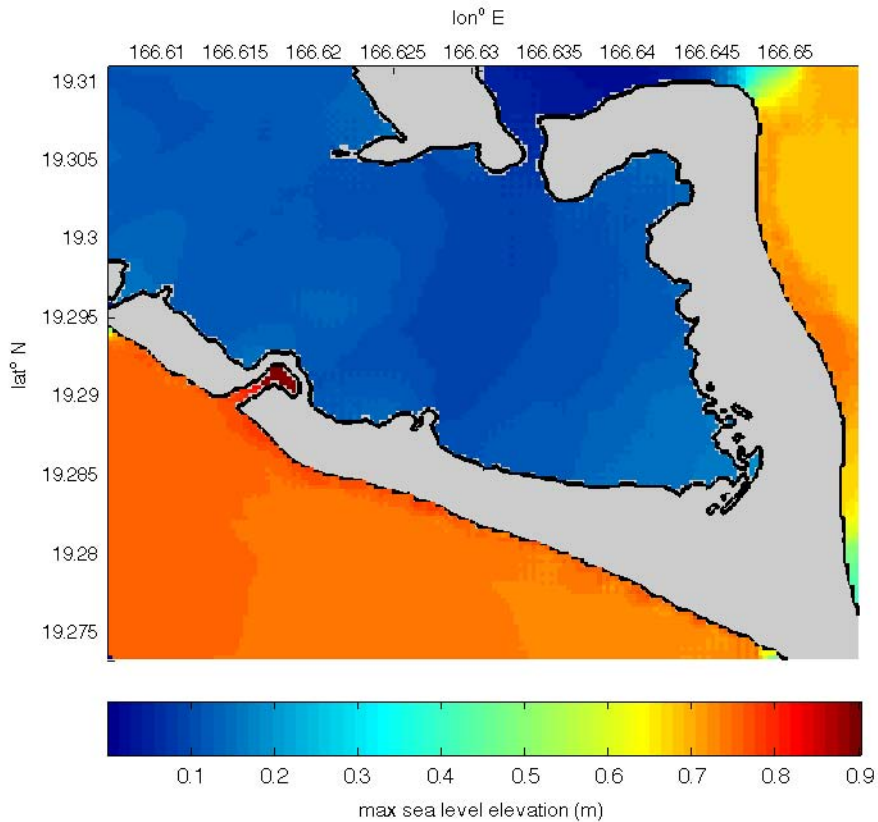




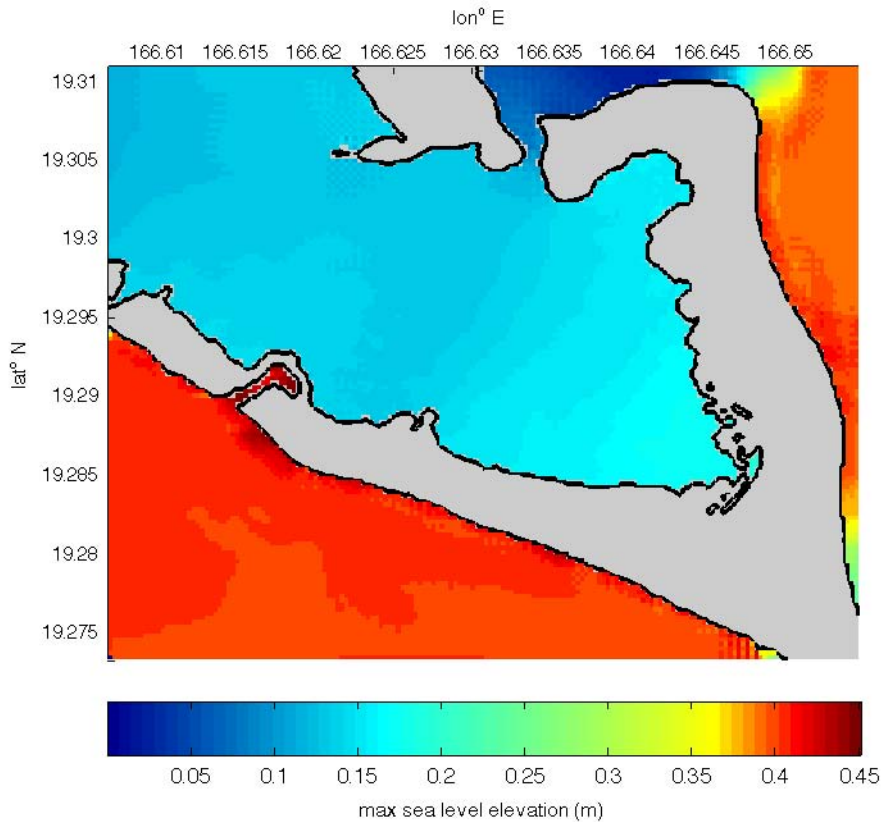


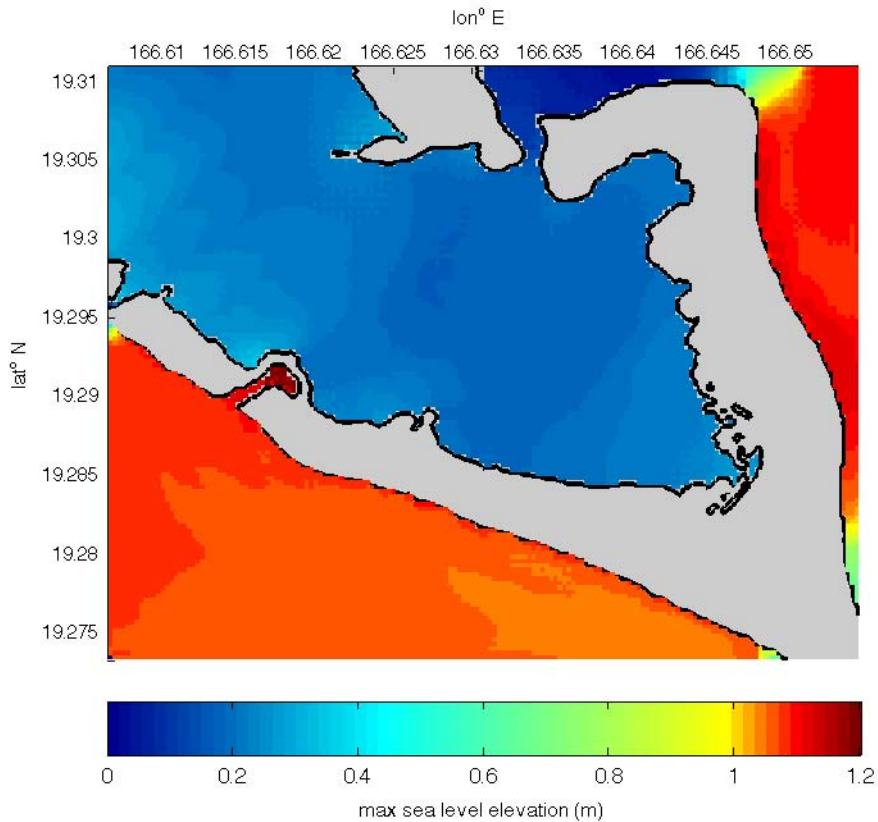


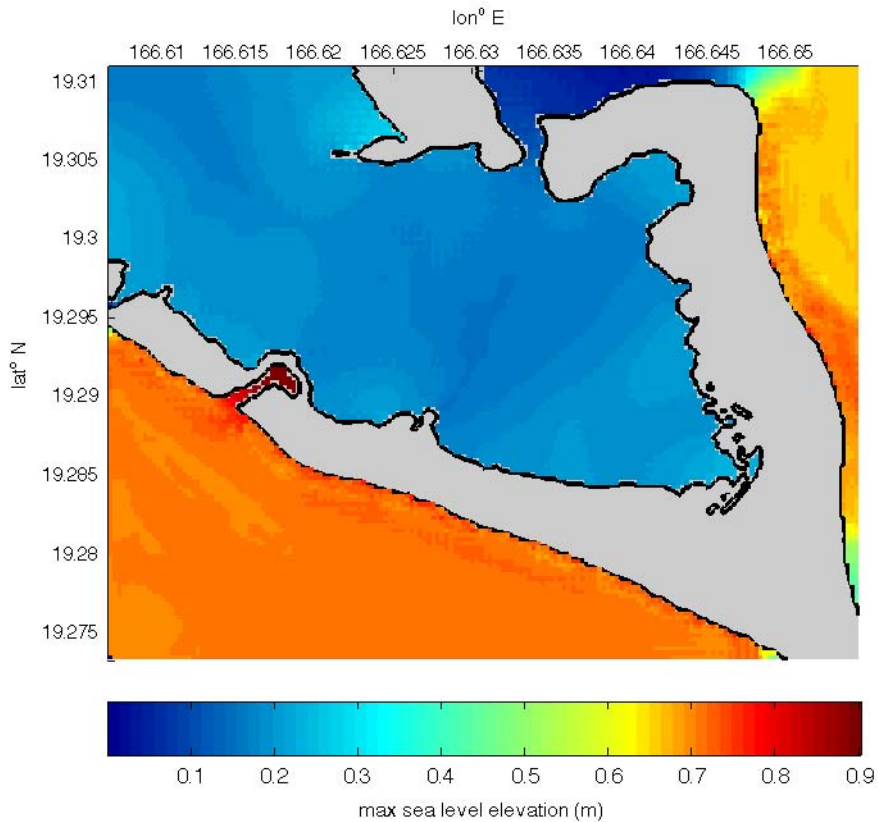


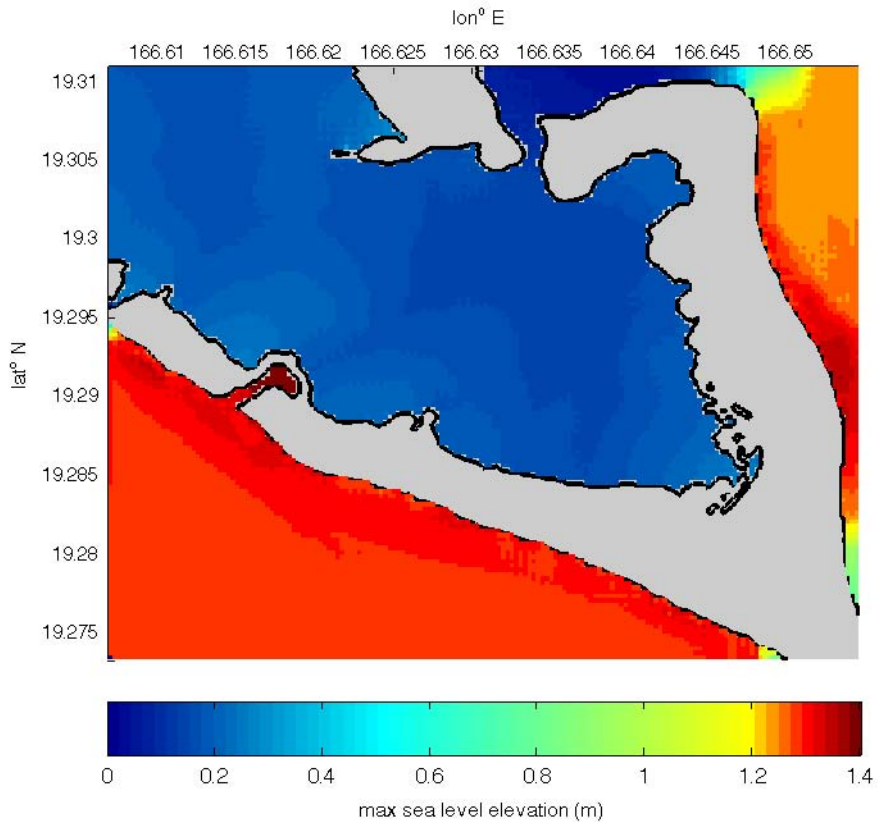


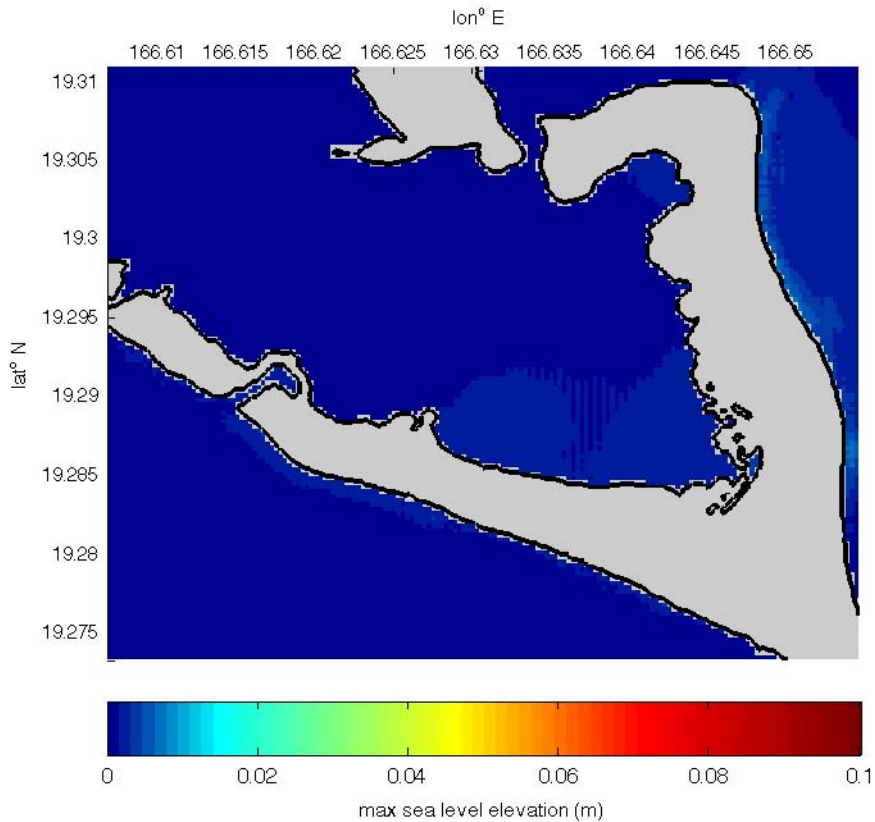


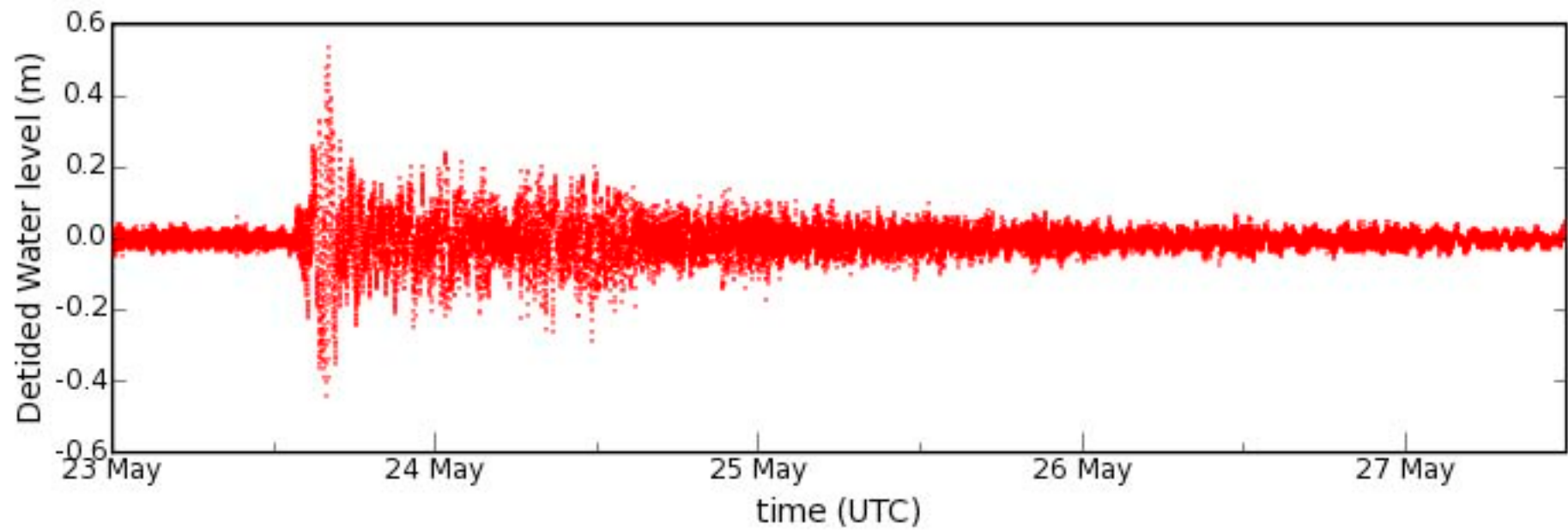


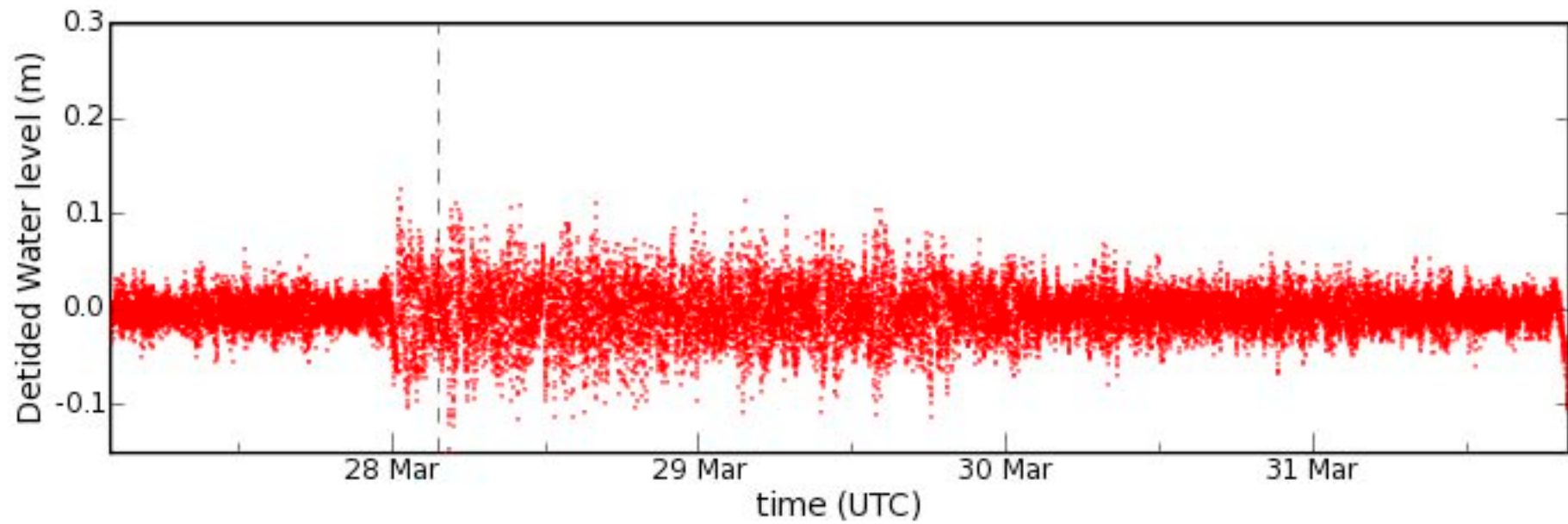




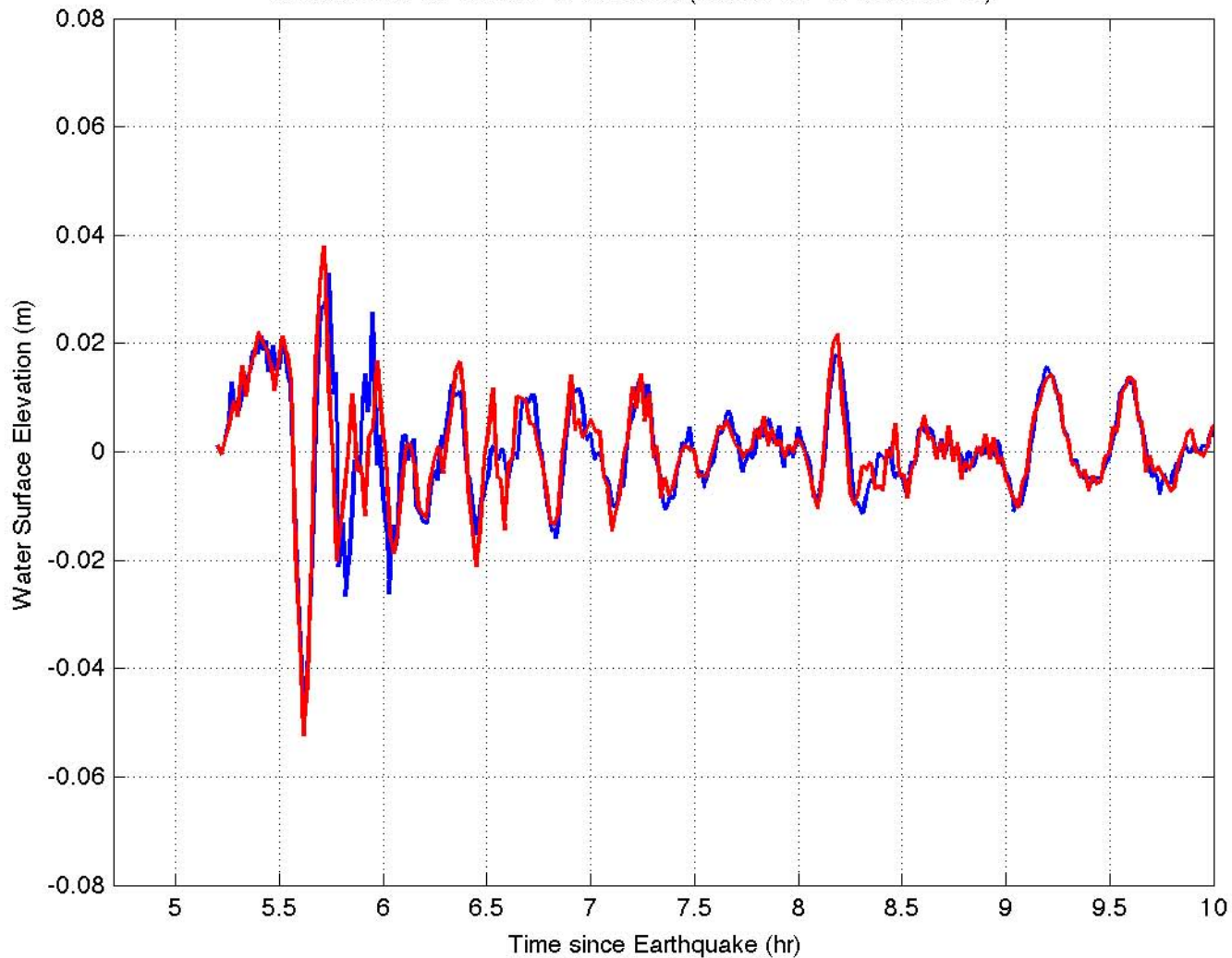






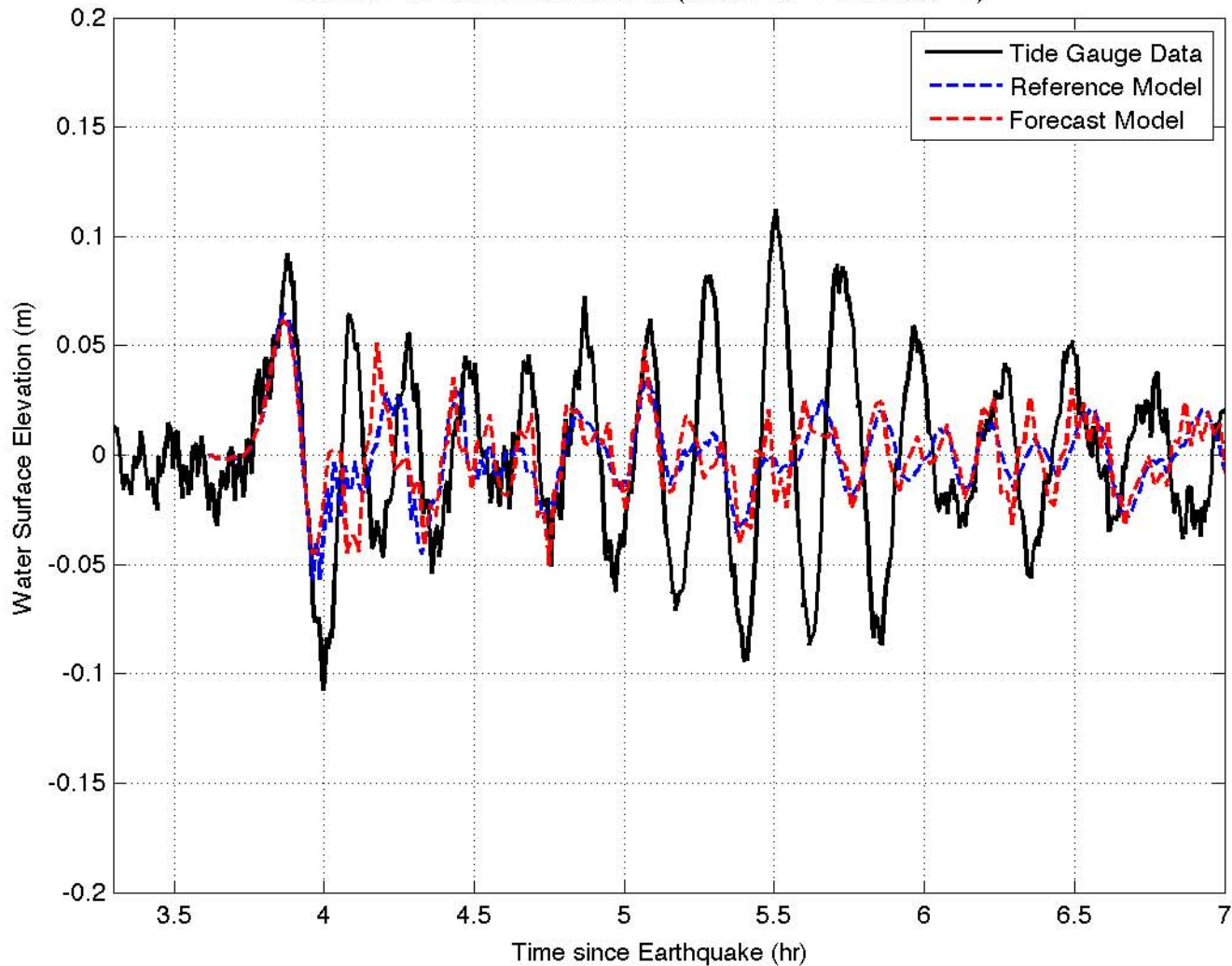


1946 Unimak Is. Tsunami at Wake Is. ( $166.6140^{\circ}$  E  $19.2895^{\circ}$  N)

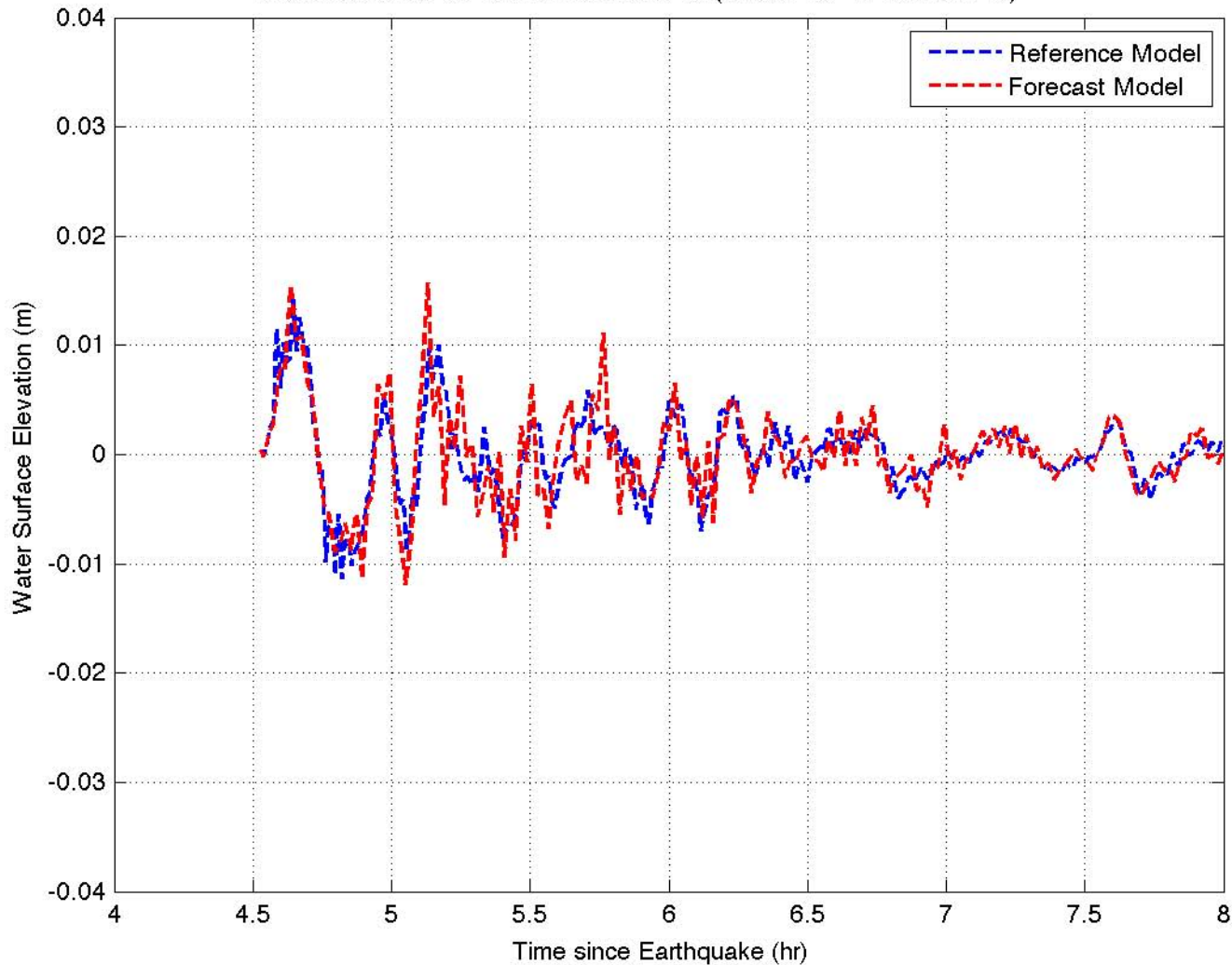




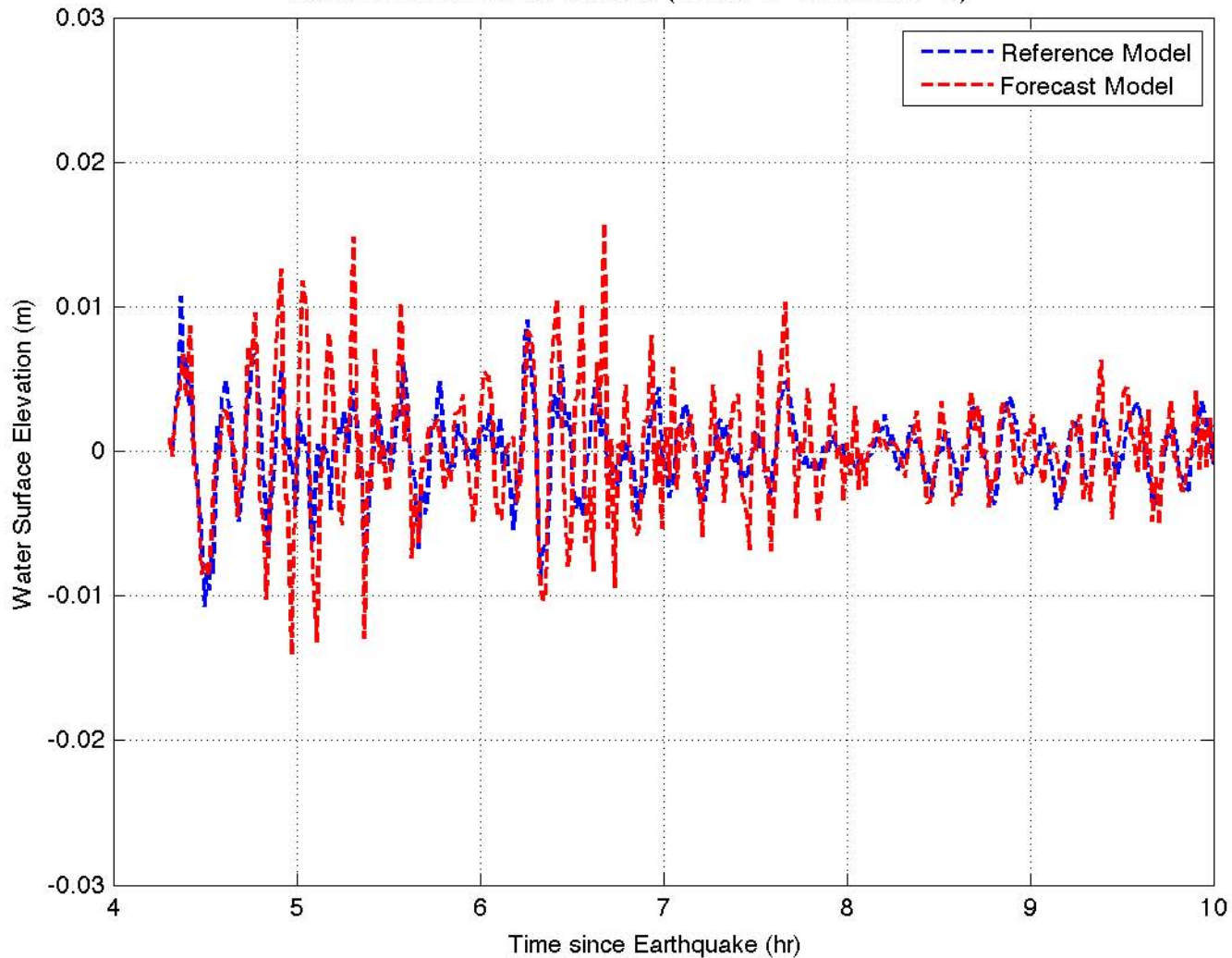
1994 Kuril Is. Tsunami at Wake Is. ( $166.6140^{\circ}$  E  $19.2895^{\circ}$  N)



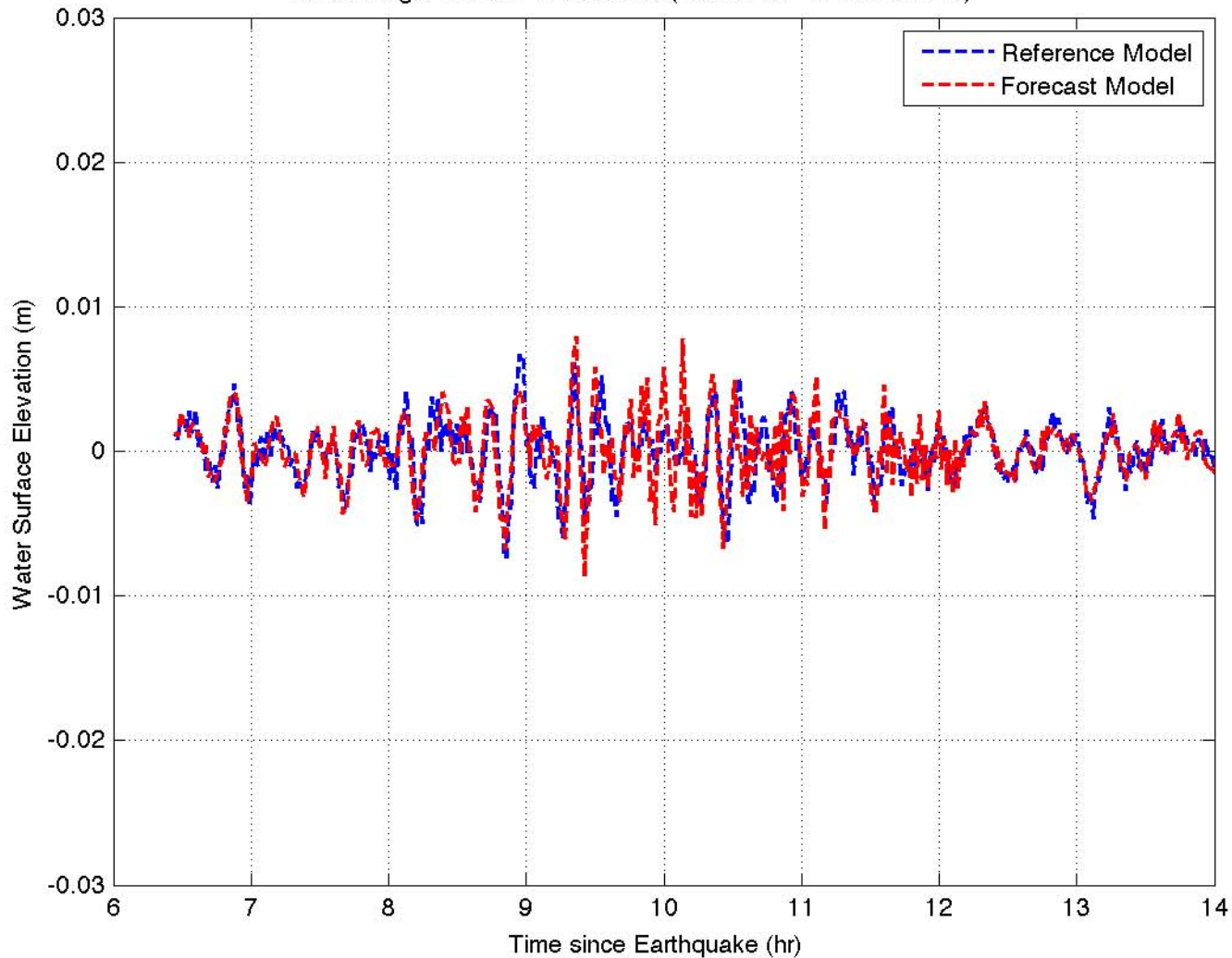
1996 Andreanov Is. Tsunami at Wake Is. ( $166.6140^{\circ}$  E  $19.2895^{\circ}$  N)



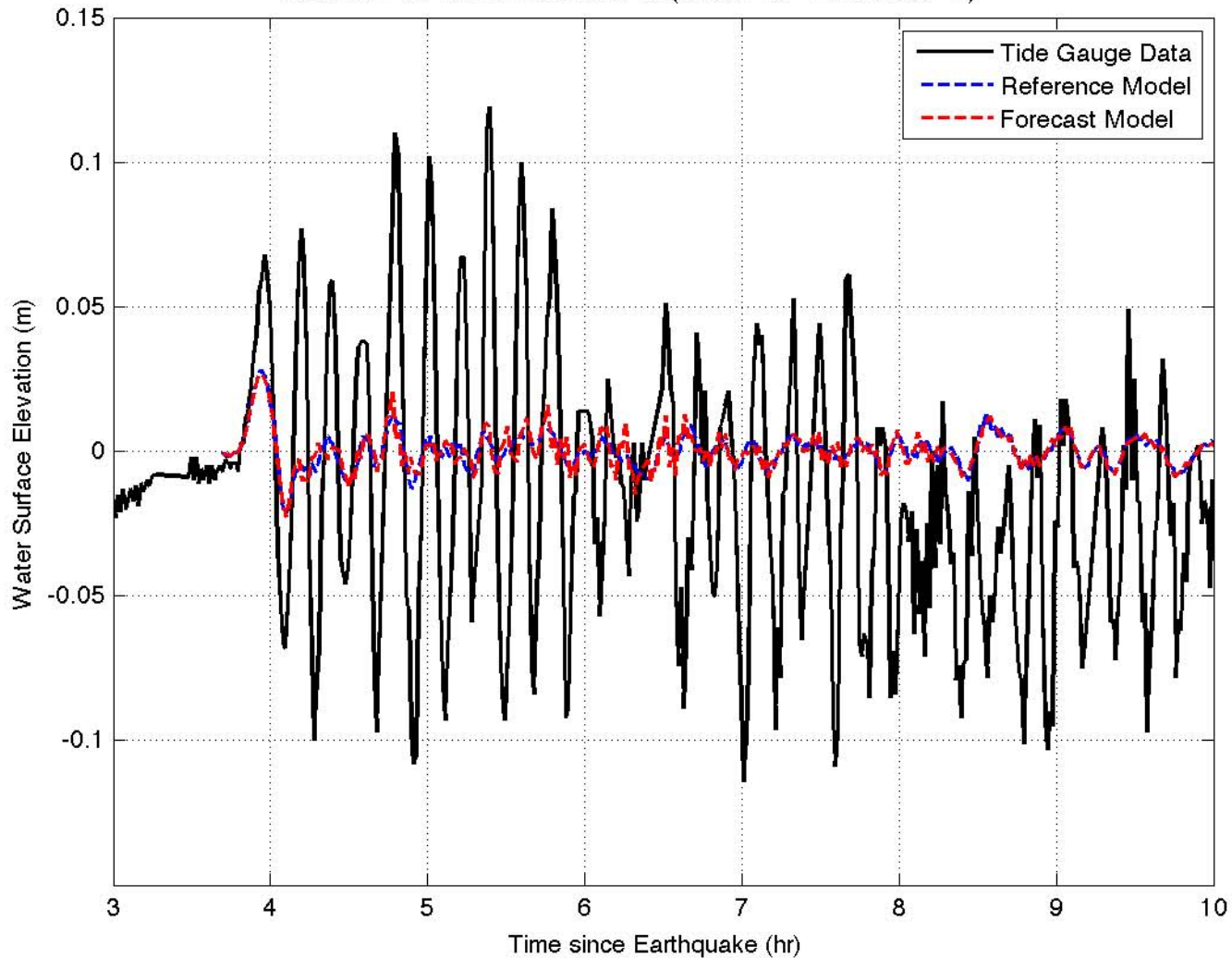
2003 Rat Is. Tsunami at Wake Is. ( $166.6140^{\circ}$  E  $19.2895^{\circ}$  N)



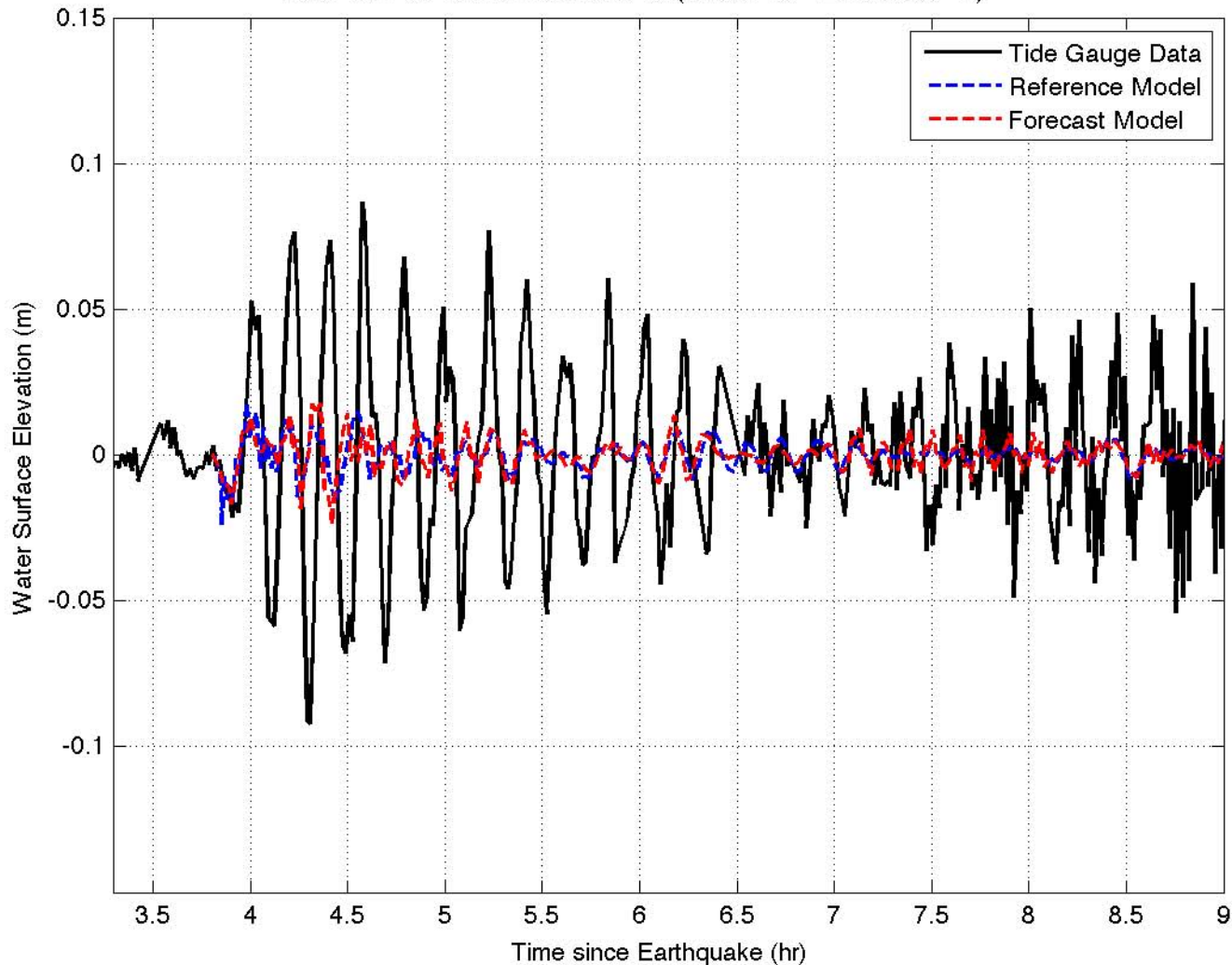
2006 Tonga Tsunami at Wake Is. ( $166.6140^{\circ}$  E  $19.2895^{\circ}$  N)



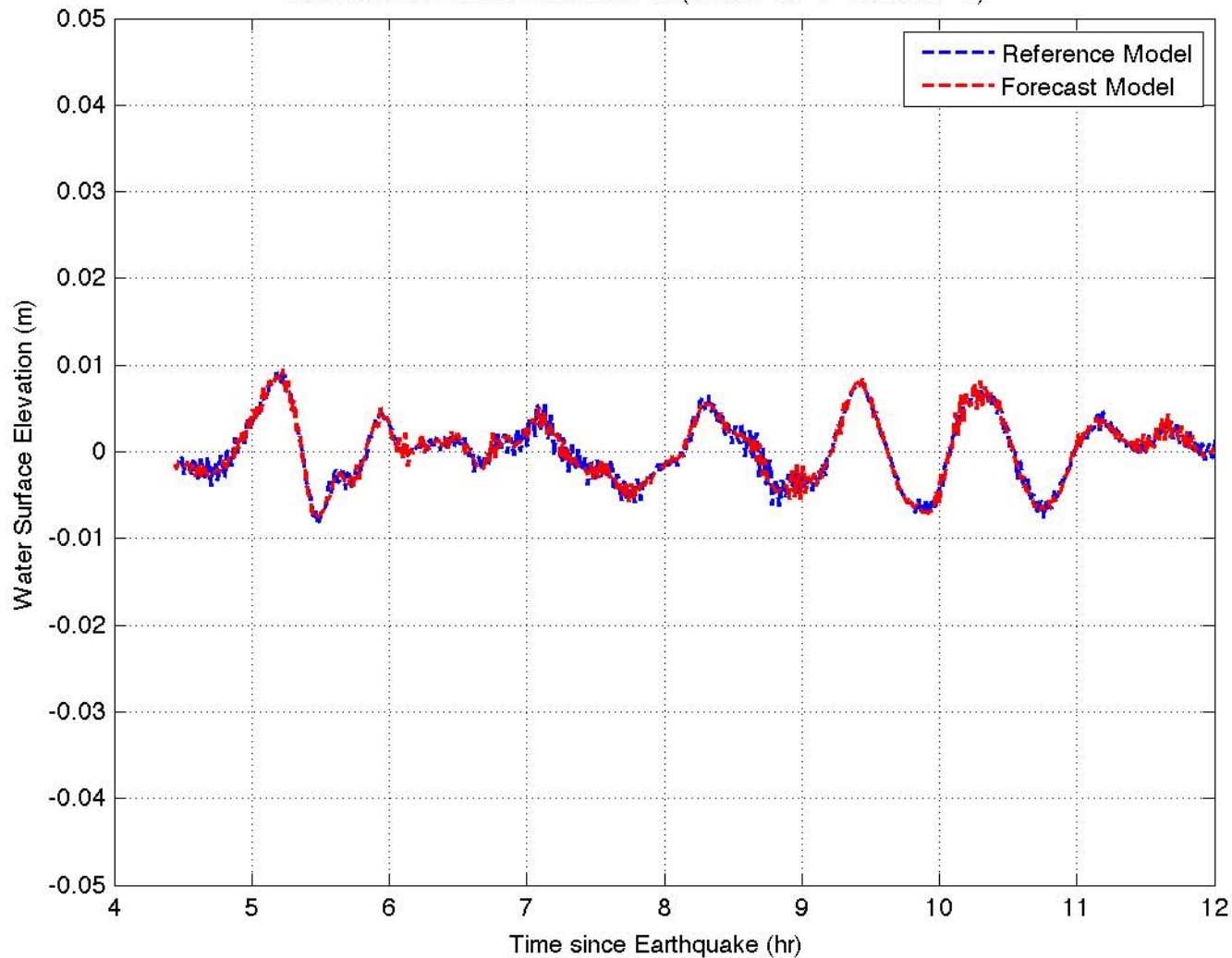
2006 Kuril Is. Tsunami at Wake Is. ( $166.6140^{\circ}$  E  $19.2895^{\circ}$  N)



2007 Kuril Is. Tsunami at Wake Is. ( $166.6140^{\circ}$  E  $19.2895^{\circ}$  N)

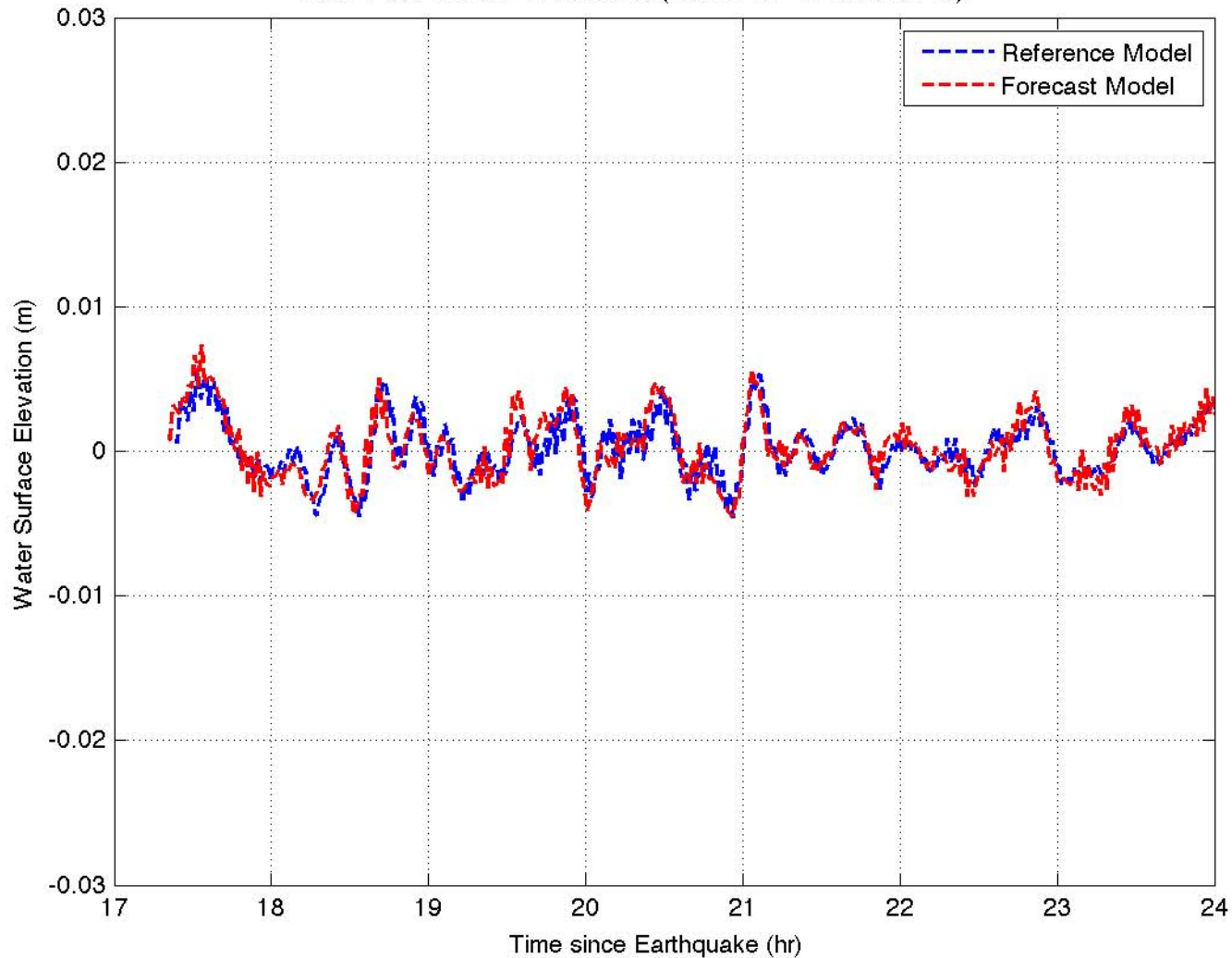


2007 Solomon Tsunami at Wake Is. ( $166.6140^{\circ}$  E  $19.2895^{\circ}$  N)



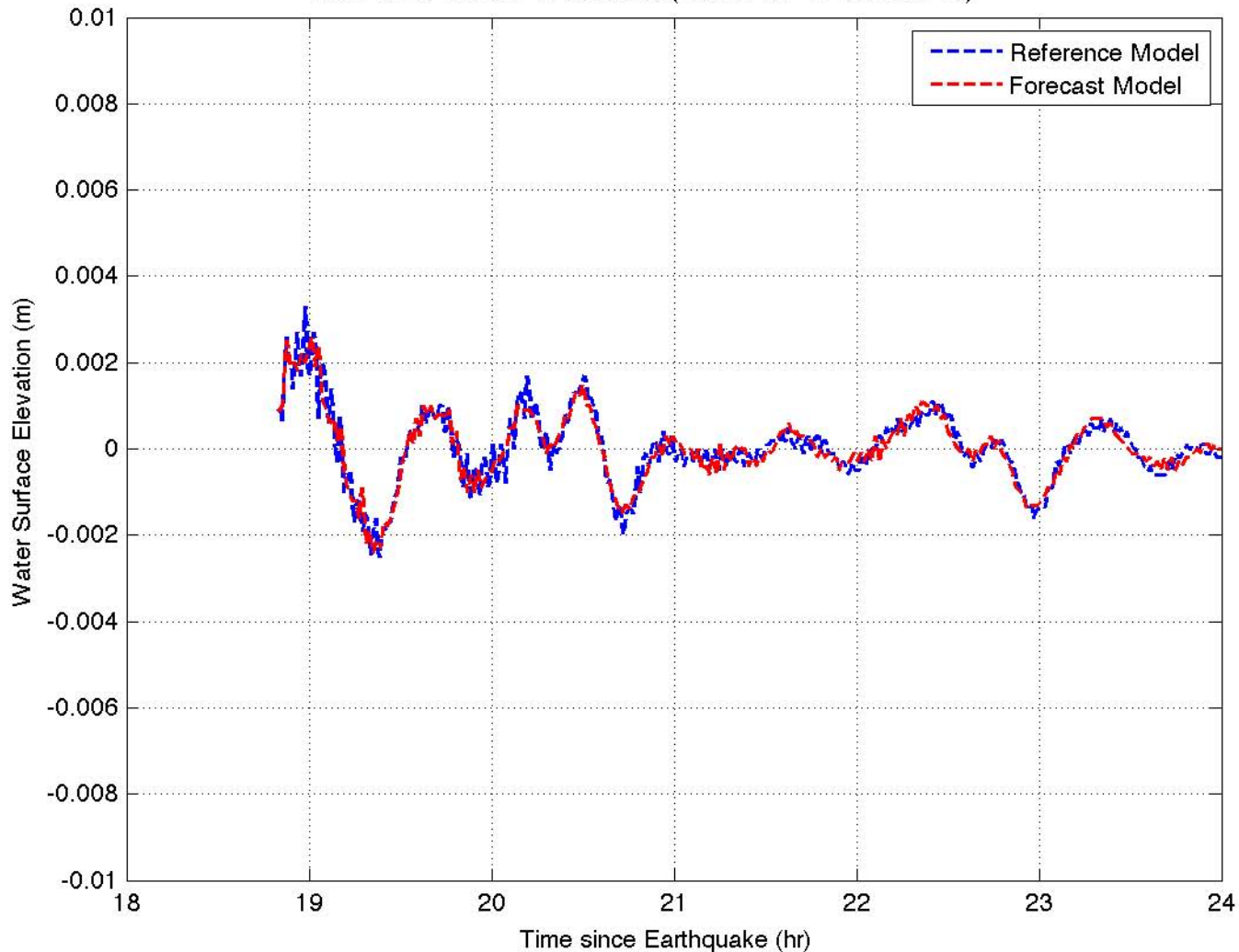


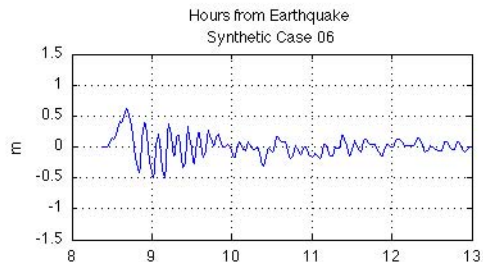
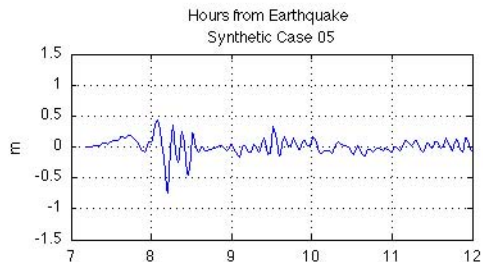
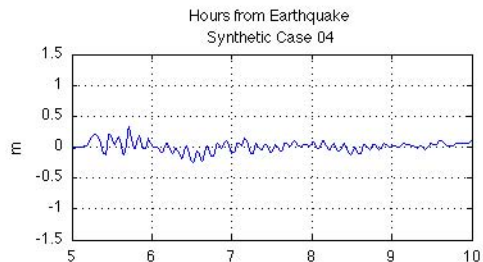
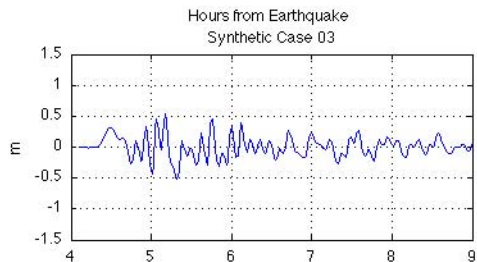
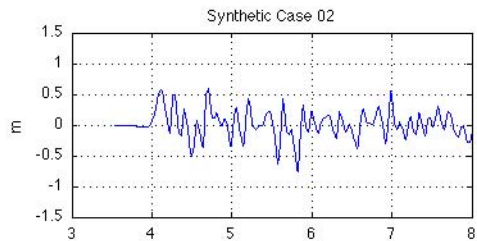
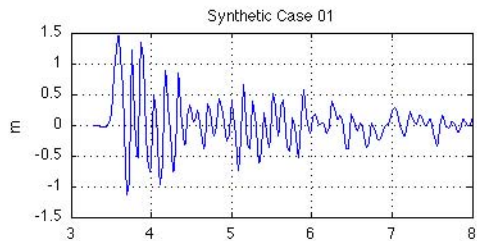
2007 Peru Tsunami at Wake Is. ( $166.6140^{\circ}$  E  $19.2895^{\circ}$  N)

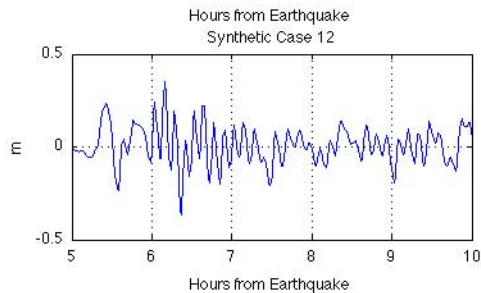
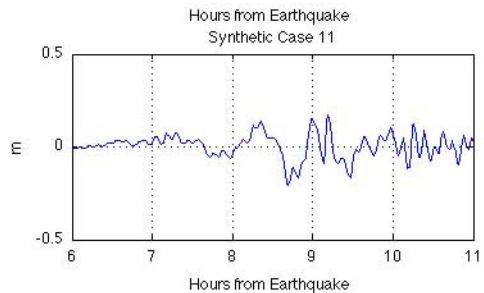
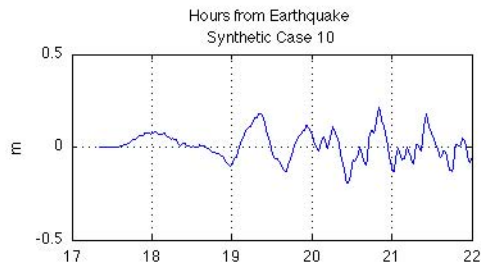
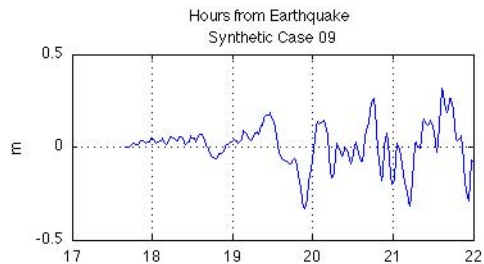
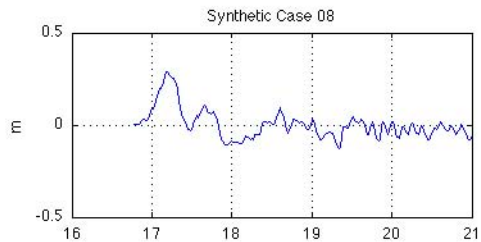
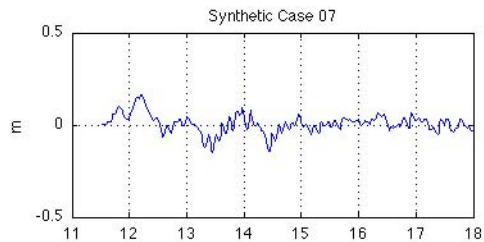


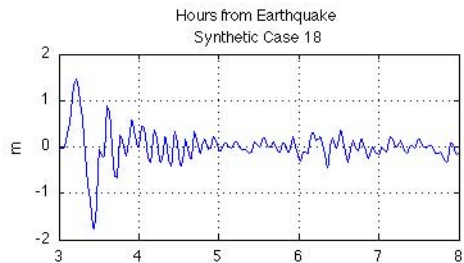
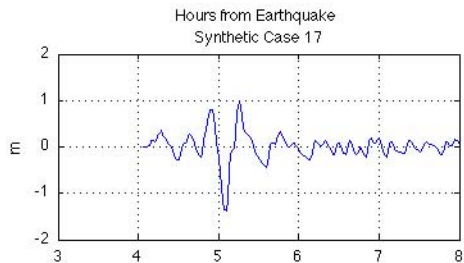
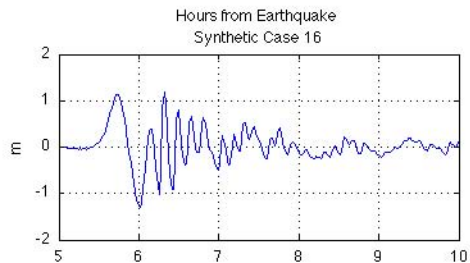
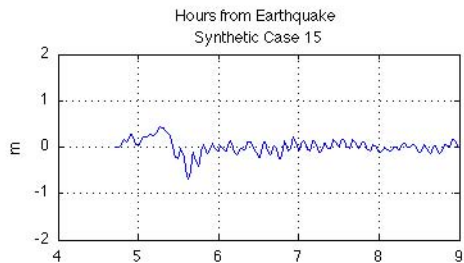
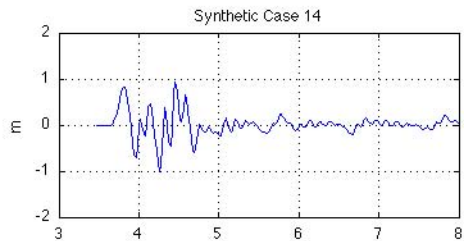
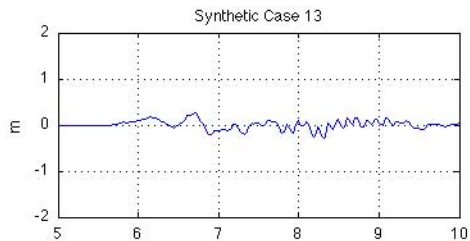


2007 Chile Tsunami at Wake Is. ( $166.6140^{\circ}$  E  $19.2895^{\circ}$  N)









Hours from Earthquake

Hours from Earthquake

## Appendix A

### A1. Reference Model \*.in file for Wake Island

0.001 Minimum amplitude of input offshore wave (m):  
1 Input minimum depth for offshore (m)  
0.1 Input "dry land" depth for inundation (m)  
0.00125 Input friction coefficient ( $n^2$ )  
1 let a and b run up  
100.0 max eta before blow up (m)  
0.27 Input time step (sec)  
320000 Input amount of steps  
12 Compute "A" arrays every n-th time step,  $n=6$   
2 Compute "B" arrays every n-th time step,  $n=$   
264 Input number of steps between snapshots  
1 ...Starting from  
1 ...Saving grid every n-th node,  $n=$

### A2. Forecast Model \*.in file for Wake Island

0.001 Minimum amplitude of input offshore wave (m):  
5 Input minimum depth for offshore (m)  
0.1 Input "dry land" depth for inundation (m)  
0.00125 Input friction coefficient ( $n^2$ )  
1 let a and b run up  
100.0 max eta before blow up (m)  
0.07 Input time step (sec)  
205000 Input amount of steps  
50 Compute "A" arrays every n-th time step,  $n=6$   
5 Compute "B" arrays every n-th time step,  $n=$   
600 Input number of steps between snapshots  
1 ...Starting from  
1 ...Saving grid every n-th node,  $n=$